AMERICAN UNIVERSITY OF BEIRUT

SPECIFIC ADHESION OF PROSTATE AND BREAST CANCER CELLS TO BONE-DERIVED MESENCHYMAL STEM CELLS AND THEIR OSTEOBLASTIC LINEAGE DIFFERENTIATION STAGE

by
NOUR ABBAS MAATOUK

A thesis submitted of the requirements
for the degree of Master of Science in Physiology
to the Department of Anatomy, Cell Biology and Physiological Sciences
of the Faculty of Medicine
at the American University of Beirut

Beirut, Lebanon
September 2020

AMERICAN UNIVERSITY OF BEIRUT

SPECIFIC ADHESION OF PROSTATE AND BREAST CANCER CELLS TO BONE-DERIVED MESENCHYMAL STEM CELLS AND THEIR OSTEOBLASTIC LINEAGE DIFFERENTIATION STAGE

BY

NOUR ABBAS MAATOUK

Approved by:

Dr. Marwan El-Sabban, Professor and Vice Chair — Advisor
Department of Anatomy, Cell Biology,
and Physiological Sciences

Dr. Wassim Abou-Kheir, Associate Professor — Member of Committee
Department of Anatomy, Cell Biology,
and Physiological Sciences

Dr. Georges Daoud, Associate Professor — Member of Committee
Department of Anatomy, Cell Biology,
and Physiological Sciences

Date of thesis defense: September 7, 2020

AMERICAN UNIVERSITY OF BEIRUT

THESIS, DISSERTATION, PROJECT RELEASE FORM

Student Name: Maatouk (Last) NOUR (First) Abbas (Middle)

☑ Master's Thesis ○ Master's Project ○ Doctoral Dissertation

☑ I authorize the American University of Beirut to: (a) reproduce hard or electronic copies of my thesis, dissertation, or project; (b) include such copies in the archives and digital repositories of the University; and (c) make freely available such copies to third parties for research or educational purposes.

☐ I authorize the American University of Beirut, to: (a) reproduce hard or electronic copies of it; (b) include such copies in the archives and digital repositories of the University; and (c) make freely available such copies to third parties for research or educational purposes after :

One ---- year from the date of submission of my thesis, dissertation, or project.

Two ---- years from the date of submission of my thesis, dissertation, or project.

Three ---- years from the date of submission of my thesis, dissertation, or project.

Signature NOUR HAMOUK Date September 17, 2020

This form is signed when submitting the thesis, dissertation, or project to the University Libraries

ACKNOWLEDGMENTS

The primordial, greatest, tremendous, long lasting thanks are for my GOD!
A CELL and a HUMAN BEING are interestingly similar. What define both are their interactions with the surrounding microenvironment. Hence, I am fortunate to be a part of such unique family and suitable niche.
I am intensely grateful to Dr. Marwan El-Sabban for being an exceptional mentor, a brilliant teacher and a patient instructor. Thank you for all your perpetual guidance. Your work credibility and delightful morals strengthened my scientific potential, and improved my prospects toward life.
I would like to express a deep appreciation to Dr. Layal El-Hajjar. Thank you for your constructive comments, help, support and encouragement.
Special Thanks go to Vera. Without you I have couldn't complete the IF Story.
I owe a very profound debt to my lab members. Moments end but memories last forever. Many sweet moments of happiness and cooperation can't be put into words.
To all the amazing people I've met on this journey, you made the fine details of this adventure.
I appreciate time spent by the committee members to read and to give comments, willing for more enhancements.
"Behind every young child who believes in himself is a parent who believed first". I have no words to say to my parents except Thank You for always being there for me!
2020 lesson: "You can't always control circumstances. However, you can always control your attitude, approach, and response".

AN ABSTRACT OF THE THESIS OF

Nour Abbas Maatouk for Master of Science
Major: Physiology

Title: Specific adhesion of prostate and breast cancer cells to bone-derived mesenchymal stem cells and their osteoblastic lineage differentiation stage.

The propensity of specific organs to harbor metastatic tumors is maintained by reciprocal interactions between cancer cells and the organ's microenvironment. Bone is the third most common site of metastasis for several solid tumors. Prostate and breast cancer cells show high affinity for bone colonization. Tumor cells extravasate from systemic circulation by adhering and traversing adjacent vascular endothelial cells. Successfully extravasated cancer metastatic cells interact with bone-lining cells that include several cell types at different differentiation states. Understanding of the molecular and cellular mechanisms that govern breast and prostate cancer cells homing to bone is an important field of research in cancer therapy that might yield novel potential targets. The overall aim of this study is to ascertain whether bone metastatic cancer cells adhere to a specific class of cells within bone tissues. We will evaluate adhesion of prostate and breast cancer cells to Mesenchymal Stem Cells (MSC) and to MSCs induced to differentiate into osteoblastic lineage at different time points. Exploring specific potential cancer cells molecules involved in initiating and maintaining adhesion to the bones is an essential step to formulate novel modalities for therapeutic intervention. We will establish an *in vitro* model of co-cultured MSC/Osteoblasts-cancer cells (Breast MDA 231 and Prostate PC 3). The system will be evaluated at different time points representing partially differentiated osteoblasts and presumably fully differentiated osteoblasts. MSCs differentiation, gene expression, protein expression and cellular localization assays will be performed, with the aim of determining the state with the highest cell-cell adhesion affinity and evaluating cancer cells-stem cells to osteoblasts interactions. The cell type with the highest adhesion affinity to cancer cells will be used to expand the co-culture system and establish more complex *in vitro* model with endothelial cells-cancer cells (Breast MDA231 and Prostate PC3) cultured on extracted bone extracellular matrix. This system, which closely mimics the bone microenvironment, will facilitate the study of cancer cell extravasation to bone and to unravel the cellular and molecular events in organ preference of metastasis.

Keywords: Metastasis, Prostate cancer, Homing, Stem cells, Organ-specific.

CONTENTS

ILLUSTRATIONS

Figure Page

TABLES

ABBREVIATIONS

CTCs: Circulating Tumor Cells

DTCs: Disseminated Tumor Cells

PMN: Pre-metastatic Niche

ECM : Extracellular Matrix

LOX : Lysyl Oxidase

JAG1: Jagged1

IL-6: Interleukine-6

VEGF: Vascular Endothelial Growth Factor

FGF: Fibroblast Growth Factor

ZO-1: Zona Occludins

CAFs: Cancer Associated Fibroblasts

MSCs: Mesenchymal Stem Cells

NKs: Natural killers

MHC II: Major Histocompatibility Complex II

Nitric Oxide Synthase: iNOS

HGF: Hepatocytes Growth Factor

MDSCs: Myeloid-Derived Suppressor Cells

TAMs: Tumor Associated Macrophages

FLT-3: FMS-Related Tyrosine Kinase 3

TADCs: Tumor-Associated Dendritic Cells

TSP1: Thrombospondin-1

ALP: Alkaline Phosphatase

PTH: Parathyroid Hormone

RANKL: Receptor Activator Of Nuclear-Factor Kappa-β Ligand

M-CSF: Macrophages Colony Stimulating Factor

MMPs: Matrix Metalloproteinases

PDGF: Platelet-Derived Factor

IGF: Insulin-Like Growth Factor

MCP-1: Monocyte Chemoattractant Protein-1

OPG: Osteoprotegrin

ATP: Adenosine Tri-Phosphate

NO: Nitric Oxide

PGE2: Prostaglandin E2

IL-1: Interleukin-1

IL-6: Interleukin-6

MIP1a: Macrophage Inflammatory Protein 1a

IL-11: Interleukin-11

PDGF: Platelet-Derived Growth Factor

AP1: Activator Protein

MAPK kinase: Mitogen Activated Protein Kinase

LPA: Lysophosphatidic Acid

PI3K: Phosphatidylinositol 3-Kinase

IFN: Interferon

EMT: Epithelial-to- Mesenchymal Transitio

CHAPTER I

INTRODUCTION

A. Cancer

Cancer is marked as the end-product of molecular and biological genetic and epigenetic modifications. Cancer is commonly classified as a major leading cause of death [1]. It is variously categorized based on the complexity of molecular pathways, stage of malignancy, and mediator's alterations or modifications [2]. Profound understanding of essential mechanisms regulating cancer colonization and spreading has been always required. "Tumor Self-Seeding" theory is proposed to explain the seeding of aggressive selected tumor cells in an optimal niche [3]. Fully competent metastatic cancer cells undergo rapid genetic modifications and phenotypic diversifications compared to benign cells and hence have a greater potential in escaping various therapeutic approaches [4],thus the need to formulate novel modalities for therapeutic intervention.

B. Seed and Soil Theory: Organ preference of Metastasis

Most of circulating tumor cells (CTCs) perishes. However, a small fraction attains their best fit destination .Organ-preference metastasis is sustained by interdependent reciprocal cell-microenvironment interactions. Based on data collection, Stephen Paget declared that the organ metastasis distribution in 735 breast cancer patients wasn't random. In 1889, Paget proposed the "seed and soil" theory to explain the propensity of specific organs to harbor metastatic tumors[5]. Indeed, for Paget

metastasis is not a hazard event, but rather, the “seed” (Tumor cells) disseminate preferentially in the appropriate, suitable “soil” (Microenvironment)[6]. Tumor malignancy is reduced when cancer cells are co-cultured with normal cells in a suitable microenvironment. Indeed, the cell’s microenvironment, despite all genetic alterations, delineates cells performance. In contrast, the anatomical/mechanical hypothesis insisted on that the metastatic secondary site is defined by the circulatory flow. Basically, mechanical theory claims that the portal venous system which is the unique venous drainage of gastrointestinal tract explain the frequently reported metastasis of gastrointestinal tumor cells into liver [7]. This theory was proposed by James Ewin in 1928 and turned later to be called “Circulation Theory” [8]. Thus, metastatic seeding in the optimal niche involves undetermined equivocal combination of mediators required for cancer cells maintenance, infiltration, proliferation and survival [9]. CTCs dissemination in a specific secondary tumor site is soil-dependent. Naturally, rich and metabolically active microenvironment guides CTCs organotropism; a well-defined distribution amid distant organs.

C. Cancer metastasis: Secondary Cancer Niche

Metastasis is classified as an inefficient process since less than 0.01% of CTCs succeed seeding the secondary tumor site [3]. A great portion of invasive and motile malignant cancer cells are released from their primary tumor site into the circulation [10]. In most solid tumors, CTCs are found in the blood stream of nearly all cancer patients but a minor fraction persists. CTCs may quit the tumor site as single cell or clusters [11]. Upon increase in their metastatic potential, CTCs infiltrate distant organs, selectively

seed the host tissue escaping immune defense, shear stress of blood flow, oxidative stress and end up residing in a new vital niche[12].Viable metastatic cancer cells homing to their new supportive organ-microenvironment are called disseminated tumor cells (DTCs). DTCs are usually drug resistant. CTCs might pursue one of two dissemination models, either metastatic linear or metastatic parallel progression. The linear model involves chronologically separated processes: invasion of primary tumor site, detachment and circulation, extravasation, latent phase of dormancy and then, invasion of the secondary tumor site. In contrast, the parallel model is characterized by an early dissemination [13-15]. Indeed, DTCs colonization of secondary tumor site is supported by dynamic interactions with the environment's extracellular matrix (ECM), immune and stromal cells creating a fertile pre-metastatic secondary niche (PMN) [16]. Alternate signaling mechanisms triggered by tumor cells hold the PMN establishment. Mixture of hypoxic cancer cells-derived secreted factors such as lysyl oxidase (LOX) a collagen crosslinking enzyme, CCL2 [17, 18], the hypoxia-induced IL-6 (Interleukine-6), [19], Notch ligand, Jagged1 (JAG1) [20]enhances the potential of the secondary site in receiving metastatic cells. Assorted heterogeneous agglomerations of signaling particles, classified as either microvessels or exosomes, play a decisive but still unclear role in promoting and handling tumor metastasis [21]. One essential and crucial step in cancer dissemination is angiogenesis [22]. Angiogenesis is the formation of new blood vessels [23]. In physiological conditions, angiogenic factors trigger pre-existing vascular vessels differentiation during embryonic development and wound healing [24]. The action of angiogenic stimuli is balanced by angiogenic inhibitors secretion[25]. However, in pathophysiological conditions like cancer, this balance is altered[26]. Angiogenic

inducers are permanently maintained whereas angiogenic inhibitors are reduced, since gaining more blood is essential for DTCs proliferation and development [22]. In addition, tumor-induced hypoxia drives basement membrane degradation through pro-anagiogenic mediators like MMPs. This will activate the migration and proliferation of endothelial cells to form new blood channels [25]. VEGF (Vascular Endothelial Growth Factor) is a potent angiogenic mediator. Besides VEGF, other angiogenic stimuli enforce new vessels formation such as TGF-β, TNF-α, FGF (Fibroblast Growth Factor) and IL-8 [27].

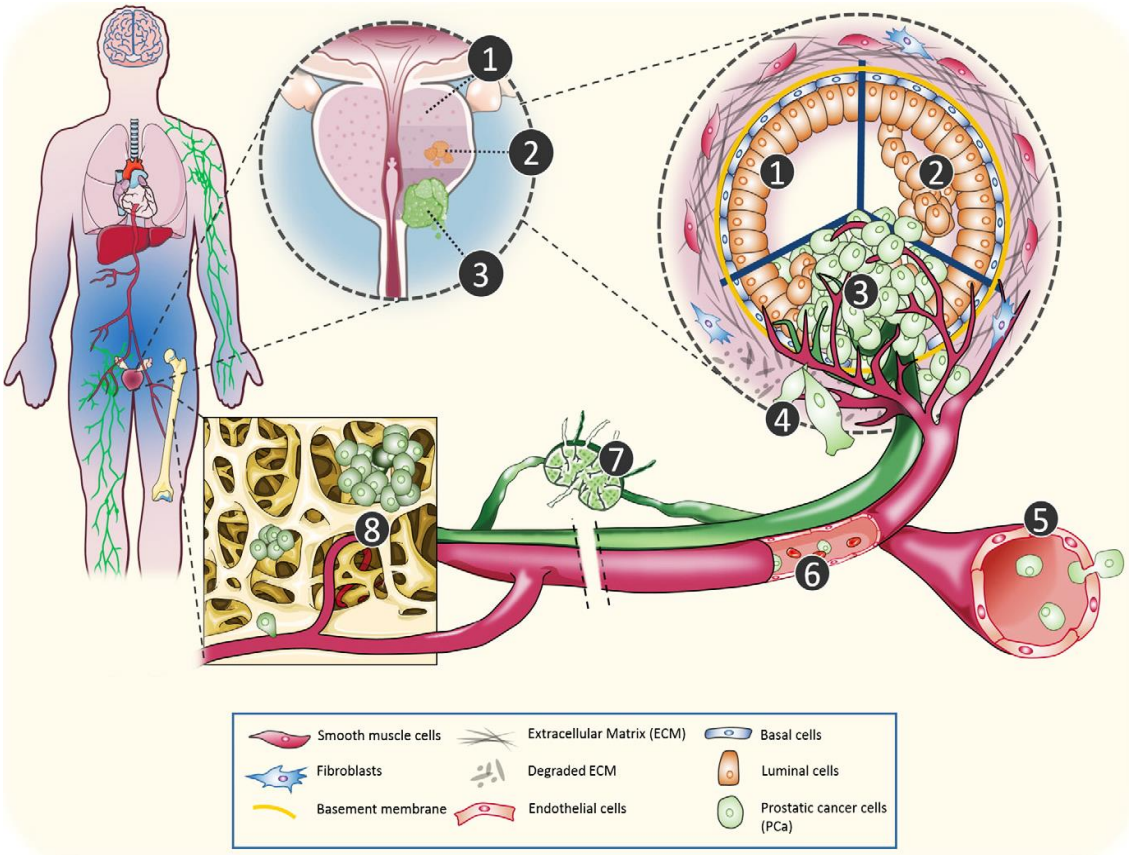

Figure 1. Schematic representation showing the consequential steps of prostate cancer cells metastasis to the bone. (1-2-3): progressive growth of prostate tumor cells in the prostatic tissue / Invasion of primary tumor site, (4): Detachment of malignant tumor cells / Epithelial to mesenchymal transition, (5-6-7): Cancer cells enter the circulation and transform into CTCs / Intravasation, (8): Arrest of CTCs / Extravasation and Invasion of the secondary tumor site.[28] After invading the primary tumor site, cancer cells detach and enter the circulation where they start being known as CTCs. After crossing several barriers, CTCs settle in a secondary tumor site and invade it as well.

D. Epithelial to Mesenchymal Transition (EMT)

Along with cancer progression, epithelial cells lose their polarity in addition to their adhesion capacities transforming into mesenchymal multipotent cells capable of differentiating into several cell types [29]. This mechanism is known as EMT. Metastatic growth induced by oncogenic-stress such as acute or chronic inflammation, promotes

EMT [30]. During EMT epithelial genes expression is altered. Dynamic EMT activates the transcription of associated genes such as Twist, ZEB, Slug and Snail [29, 31]. Slug and Snail have both been involved in the up-regulation of MMPs. Thus, tumor cells acquire mesenchymal features and develop invasive characteristics that promote their detachment, migration and invasion. Indeed, epithelial cells modify their apical-basal polarity, re-arrange their cytoskeletal system and lose their cell-cell adhesion [30, 32, 33]. Furthermore, epithelial markers such as E-cadherin, Claudins and zona occludins (ZO-1) are replaced with mesenchymal markers, mainly N-cadherin, vimentin and fibronectin enhancing cell motility and migration potential [34, 35]. EMT is accompanied with the "Cadherin Switching" phenomenon between the epithelial E-cadherin and the mesenchymal N-cadherin expression. EMT is usually associated with chronic inflammation [36]. Within a chronically inflamed microenvironment, tumor infiltrating immune cells secretes cytokines and chemokine such as TGF-β, TNF-α and activates nuclear factor kappa B (NF-κB), Notch, Wnt, and Hedgehog signaling pathways [37, 38]. Activation of Wnt pathway results in the translocation and accumulation of β-catenin in the nuclear compartment which is reported in cells undergoing EMT [39]. In addition, cancer associated fibroblasts (CAFs) originate from bone marrow mesenchymal stem cells (MSCs), fibroblasts and epithelial cells trans-differentiation [40]. A study has shown that MSCs and CAFs share many expressed surface markers, mainly CD29, CD44, CD73, CD90, CD106 and CD117[41]. Another recent review described the MSCs as resting fibroblasts[26]. Once activated, their secretion and proliferation capacities increase. Fibroblasts secret higher amounts of TGF-β, VEGF, IL-4, IL-10 and TNF-α compared to MSCs [42]. MSCs-CAFs common characteristics might also support that

CAFs are MSCs derived cells. Cancer associated fibroblasts secret pro-inflammatory cytokines contributing to EMT maintaining and cancer progression [43, 44]. CAFs activation rise cancer aggressiveness by recruitment of immune cells and maintain angiogenesis support [2]. Moreover, EMT is reversible. Mesenchymal cells can revert back into their epithelial state forming clusters of metastatic growth [45]. MSCs interactions with malignant epithelial cells promote cytokines and growth factors release which promotes epithelial cells motility [46] .EMT is also regulated by miRNAs. MiR-200 family's post translational ability to regulate the molecular pathways of several transcription factors suppress the expression of ZEB1 and ZEB2 [47]. In the opposite direction, ZEB establish a "double negative feedback loop" to reinforce their expression and maintain the transition between the epithelial and mesenchymal states [29].

E. Escaping Immune Defense

In the first stages of cancer development, infiltrating immune cells fulfill an anti-tumor activity. However, immune cells' interactions with tumor microenvironment, especially with resident stromal cells switch their behavior[48]. Indeed, dynamic but also complex immune interactions have shifted the adopted thoughts concerning immune system surveillance in metastatic malignant cancer. Natural killers (NKs) and cytotoxic T cells are initially fundamental anti-tumor mediators. However, complicated mixtures of pre-existing and recruited immune cells interactions with tumor microenvironment generate potent tumor-promoting activities of immune cells [49].NKs and cytotoxic T cells start expressing a variety of pathological mediators such as arginase, inducible

nitric oxide synthase (iNOS), TGF-β, IL-10, and cysteine [41, 50, 51]. Tumor cells not only escape immune supervision, but also use cytokines and direct interactions with immune cells to promote tumor outgrowth and expansion [52]. Escaping mechanisms include mainly antigen loss or deregulation in antigen presentation and down-regulation of major histocompatibility complex (MHC II) [53]. In addition, inflammatory microenvironment switches the normal anti-tumor function of MSCs into immune-suppressive cells, inducing a stressed phenotype caused by DNA damage [46]. Immune-suppressive MSCs alter T cells functions by the secretion of TGF-β and hepatocytes growth factor (HGF), and indoleamine 2,3-dioxygenase which promote the apoptosis of activated T cells [54]. Cancer cells also recruit mast cells, Dendritic cells (DCs), tumor associated macrophages (TAMs) and myeloid-derived suppressor cells (MDSCs) by chemokines and cytokines secretion and use them to support the survival and growth of tumor mass [2]. Under normal physiological conditions, hematopoietic stem cells differentiation into common myeloid progenitor and immature myeloid cells is triggered by a collection of cytokines mainly M-CSF, IL-3, and FMS-related tyrosine kinase 3 (FLT-3). In peripheral organs and tissues, further differentiation generates mature dendritic cells, monocytes and macrophages. However, pathophysiological transformations switch these progenitor cells into MDSCs [55, 56]. Moreover, MDSCs become the source of different cell lineages like tumor-associated dendritic cells (TADCs), tumor-associated neutrophils (TANs), TAMs.

F. Vascular Bone Niche and Endothelial cells

Blood is a critical microenvironment for CTCs. Risky factors such as physical shear stress; oxidative stress and immune surveillance narrow the CTCs survival and restrict their arrest at the distant suitable niche. Tumor cells secret thrombin, cathepsin B, cancer procoagulant, and MMP to outstrip danger and maintain their survival in the vasculature. Tumor cells also induce platelets aggregation and selectin up regulation which helps in facilitating their extravasation at distant organs [57]. Under circulatory stress, CTCs undergo apoptosis-like phenomena called anoikis due to loss of ECM adhesion markers, initially integrin which is essential for their survival [58]. A minor portion of CTCs compensate either by controlling their glucose uptake through the activation of pentose phosphate pathway or by the activation of tyrosine kinase-dependent pathways [59]. Another factor to be considered is the difference in size between CTCs which is an average of 20-30μm and the diameter of a capillary which is approximately 8μm. This fact increases the probability for CTCs to become trapped in capillary beds along with their circulation journey [46]. Reaching the optimal distant organ, few primary tumor cells confront the first impediment which are endothelial cells supported by smooth muscle cells and pericytes in the vascular bone marrow niche. CTCs aggregations bind to the endothelium and might block it. Bone colonization is initiated by tumor cells-endothelial barrier interactions. Vascular permeability is indispensable for extravasation. It is achieved by CTCs released factors like angiopoietin [60]. Indeed, binding of the extracellular chemokine CXCL12 to the cell surface receptor CXCR4 facilitates tumor cells-endothelium attraction and adhesion [61,

[62]. It has been shown that CXCL12 is commonly expressed at different metastatic sites such as: lung, liver, bone marrow and brain. Adhesion molecules such as E-selectin ligand, b1 integrin, and Rac1 promote cancer cells –endothelial cells intercommunication [63, 64] **.** Hence, loss of E-Selectin expression, disrupt prostate cancer potential to adhere to bone endothelial cells through E-selectin receptor (also known as CD62E or ELAM-1) [65]. In addition, Ghajar and Colleagues showed that metastatic cells prefer homing into the perivascular niche where they maintained held by endothelial cells via thrombospondin-1 (TSP1) rather than endosteal niche [47]. Intravasation and extravasation are both controlled by the anatomical and structural characteristics of the endothelial barrier. Indeed, alteration of endothelial permeability facilitates cancer spreading.

G. Physiology of Bone microenvironment _ Bone niche

Bone maintains the body's anatomical and structural support. Tumor microenvironment consists of infiltrated immune cells, mesenchymal stromal cells, vasculature and extracellular matrix [66].Mesenchymal stromal cells include : mesenchymal stem cells, pericytes, fibroblasts and osteoblasts [67]. Bone is a dynamic tissue with a particular homeostatic remodeling continuously balanced by osteoblastic deposition and osteoclastic resorption[68]. Metabolically active bone cells reside on a definitive ECM that provides biochemical and fundamental dynamic uphold of bone constituents [69]. Osteoblasts contribute for the major portion of ECM proteins secretion, essentially collagen I, an organic predominant protein, alkaline phosphatase (ALP) and osteocalcin and hydroxyapatite, inorganic mineralization protein, handling the plasticity

but also durability of bone[70]. Additionally, bone osteoblasts are MSC-derived cells. Thus, Runx2 and Osterix are master genes expressed regularly by osteoblasts [70].MSC-induced osteogenesis and adipogenesis have been shown to be conversely related. Indeed, paracrine factors essentially parathyroid Hormone (PTH) and Wnt guide MSC differentiation into osteoblasts[71]. Once osteoblasts are trapped within the matrix they secret, they become less metabolically active cells called osteocytes, also known as the mechano-sensory bone cells[70]. Inactive osteoblasts residing on the bone surface are known as lining cells also known as bordant cells [72]. However, osteoclasts, derived from the fusion of 30-50 hematopoietic stem cells nuclei in the bone marrow, are characterized with an acidic lacuna _ Howship (pH = 5.5) by which they break down bone ECM [73].

Through bilateral interactions, bone cells achieve mutual survival. The oseoblastic receptor activator of nuclear-factor kappa-β ligand (RANKL) can be found in bound or soluble form .RANKL is activated via osteoprotegerin also secreted by osteoblasts via an autocrine signaling pathway .Osteoblasts also secret macrophages colony stimulating factor (M-CSF). RANKL and M-CSF are crucial for osteoclastic maturation and differentiation[74, 75]. Osteoblasts-derived MMPs (Matrix Metalloproteinases) are also notable ECM non-collagenous proteins effectively active in bone matrix dissolving [76].

Bone homeostasis is accomplished by cellular functional balance (Figure2). Many hormones regulate bone remodeling, such as PTH, estrogen and calcitonin [77]. In effect, PTH interacts with G-protein-coupled osteoblastic receptor and modulates serum calcium concentration [78]. Osteocytes apoptosis due to injury in the bone

microenvironment stimulates osteotropic factors secretion and cytokines release which activate osteoclastogenesis . TGF-β, PDGF (platelet-derived factor) and IGF (insulin-like Growth Factor) adjust bone homeostasis and osteoclasts activation. Intracellular calcium signaling pathway activates the recruitment of hematopoietic cells and their differentiation into bone resorption cells by monocyte chemoattractant protein-1 (MCP-1) release. Simultaneously, osteoblastic-derived, RANKL's decoy receptor osteoprotegrin (OPG) is down-regulated increasing osteoclastic formation and M-CSF and RANKL expression. Additionally, osteoclastic attachment to the unminerilized osteoid bone matrix is maintained by osteoblastic MMPs. On the bone surface, attached osteoclasts establish an acidic "Howship's resorption lacunae" rich with H+ ions and proteolytic enzymes dissolving the mineral matrix [79]. Resorption phase is confined by a formation equivalent phase [80]. Osteoblasts activation is the sub-sequential event of osteoclasts apoptosis. Resorption gaps are fulfilled by osteoid matrix produced by osteoblasts. Osteocytes are also involved in bone formation by the production of prostaglandin E2 (PGE2), nitric oxide (NO) and adenosine tri-phosphate (ATP) enhancing osteoblasts activation [81]. In contrast, RANK/OPG axis is altered during metastasis-induced local inflammation.

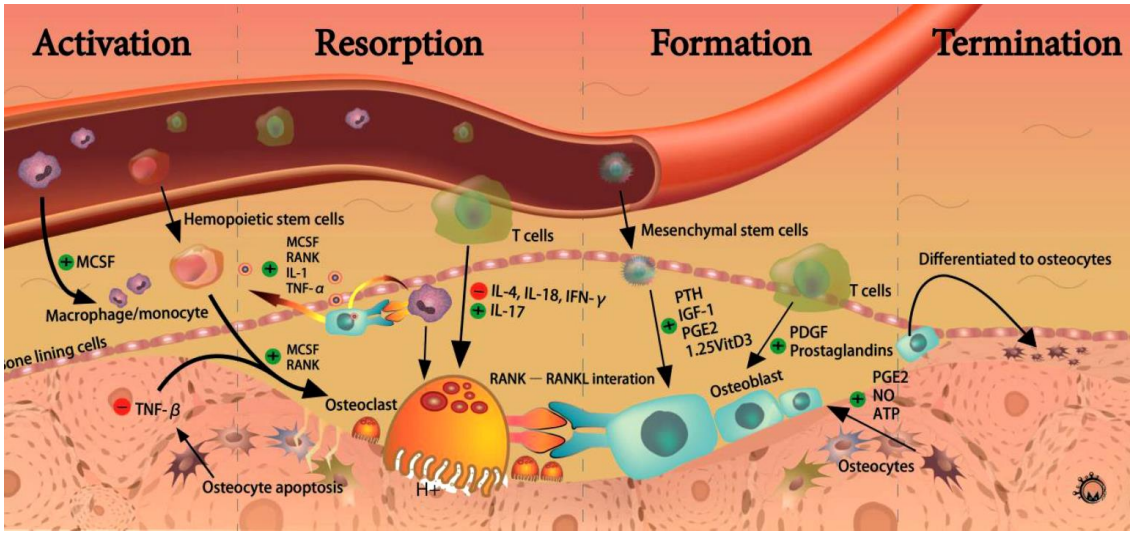

Figure2. Schematic presentation of the consequential steps of bone remodeling and the variety of activated molecular pathways [82].

H. Bone Microenvironment during metastasis

Bone is the third most common site of metastasis for several solid tumors [83].What makes bone tissue a preferred site for metastatic cancer cells homing is the permanent release of growth signals due to continuous constant turn over which are pivotal for cancer cells survival in the microenvironment[84]. Indeed, CTCs dissemination and outgrowth are controlled by glut of cytokines and growth factors secreted by bone microenvironment cells, essentially hematopoietic and mesenchymal stem cells, endothelial cells, osteoblasts and osteoclasts [10]. The existence of endosteal and perivascular niche supplying bone with blood flow via vascular sinusoids favors bone for metastasis [23]. Bone oxygen levels fluctuate from <1% to 6% creating a hypoxic microenvironment suitable for cancer cells colonization [85]. Each step in the metastatic cascade requires cell-cell and cell-ECM interactions [86]. Basically, prostate

and breast metastatic cells express integrin in order to adhere to bone ECM, and to osteoblasts and osteoclasts via vitronectin and osteopontin [87].

At the genetic level, 102 metastatic genes were stated [88]. Reported genes entangle in bone marrow invasion (CXCR4), ECM degradation (MMPs, ADAMTS1, and Proteoglycan-1), and angiogenesis (VEGF, FGF5) [27]. Several other bone metastatic genes were described [72]. Epigenetic modifications alter genes expression and increase pathways complexity [89-91]. Additionally, metastatic incidence increases with age, this is associated with the accumulation of several oncogenic mutations of an individual's lifetime [1]. However, gene distinctive overlaps with unknown genes along with cancer heterogeneity has not yet contributed to definite explanation for cancer dissemination mechanism [92]. Cancer niche development can be divided into three stages: construction, expansion and maturation. Early, transformation of normal cells into cancer cells is the initial result of their interactions with stromal cells. Then, tumor spreading is regulated by the release of a variety of factors such as chemokines, cytokines and exosomes. Afterwards, resident cells recruitment, especially fibroblasts induces microenvironment maturation. In effect, a dynamic niche is chemical promoters - dependent where the construction of suitable microenvironment is supported by the stromal composition. Stromal cells recruitment is mediated by the activation of several molecular pathways including mitogen-activated protein kinase (MAPK), STAT3 and β-catenin pathways.

I. Mesenchymal Stem Cells and Pre-metastatic Niche in Bone

Bone and blood progenitor cells reside in the bone marrow of trabecular (spongy) bone[8]. Bone marrow is the proliferative niche rich in MSCs responsible for bone homeostasis, in addition to HSCs recruitment and maturation. At the physiological level, MSCs serve as progenitor multipotent cells with high self-renewal potential[93]. The three main MSCs sources are: bone marrow, adipose tissue and dental pulp [94-97]. MSCs contribute to bone turn-over by differentiating into several cell lineages such as osteoblasts, chondrocytes and adipocytes. MSCs are positive for mainly three surface markers: CD73, CD105 and CD90 [98] and express mainly CXCL12 [99], Nestin [67] and neuron glial antigen 2 (NG2) [100]. Mesenchymal stromal cells provide fundamental factors to sustain the microenvironment's homeostasis. HSCs recruitment is monitored by HSCs interactions with osteoblasts steeled in the endosteal niche and mesenchymal/endothelial cells in the perivascular niche [101]. However, competition between HSCs and tumor cells shifts the microenvironment where mesenchymal stromal cells reside to a pre-metastatic niche favoring tumor outgrowth, [102] release pro-metastatic and angiogenic factors, stimulate tumor cells invasion and migration by creating an immunosuppressive niche, maintaining EMT [63] and MSCs differentiation into CAF [103]. Commonly, a very minor number of DTCs succeed to colonize the secondary tumor site giving rise to metastatic lesions. To persist, metastatic cells require a cascade of molecular pathways activation and adhesion molecules expression holding pre-metastatic niche formation (Figure3). Thus, MSCs promote tumor cells survival or dormancy via a variety of mediators [104]. Dormancy can be divided into three

categories. Cellular dormancy where DTCs enter a phase of quiescence, angiogenic dormancy where blood vessels interrupt the metastatic invasion and the immune dormancy where tumor mass is kept under surveillance. From different perspective, Barcellos-Hoff et al suggested that pre-metastatic niche formation is an essential requisite for tumorigenesis [48]. Cancer interactions with the surrounding stroma diverge the microenvironment toward an inflammatory active state well-supplied with cytokines and growth factors [105]. Tumor inflammation is a "wound that never heals". The dynamic inflammatory milieu is suitable for MSCs and other cell lineages recruitment [106]. Circulatory MSCs home to inflammatory sites [107].

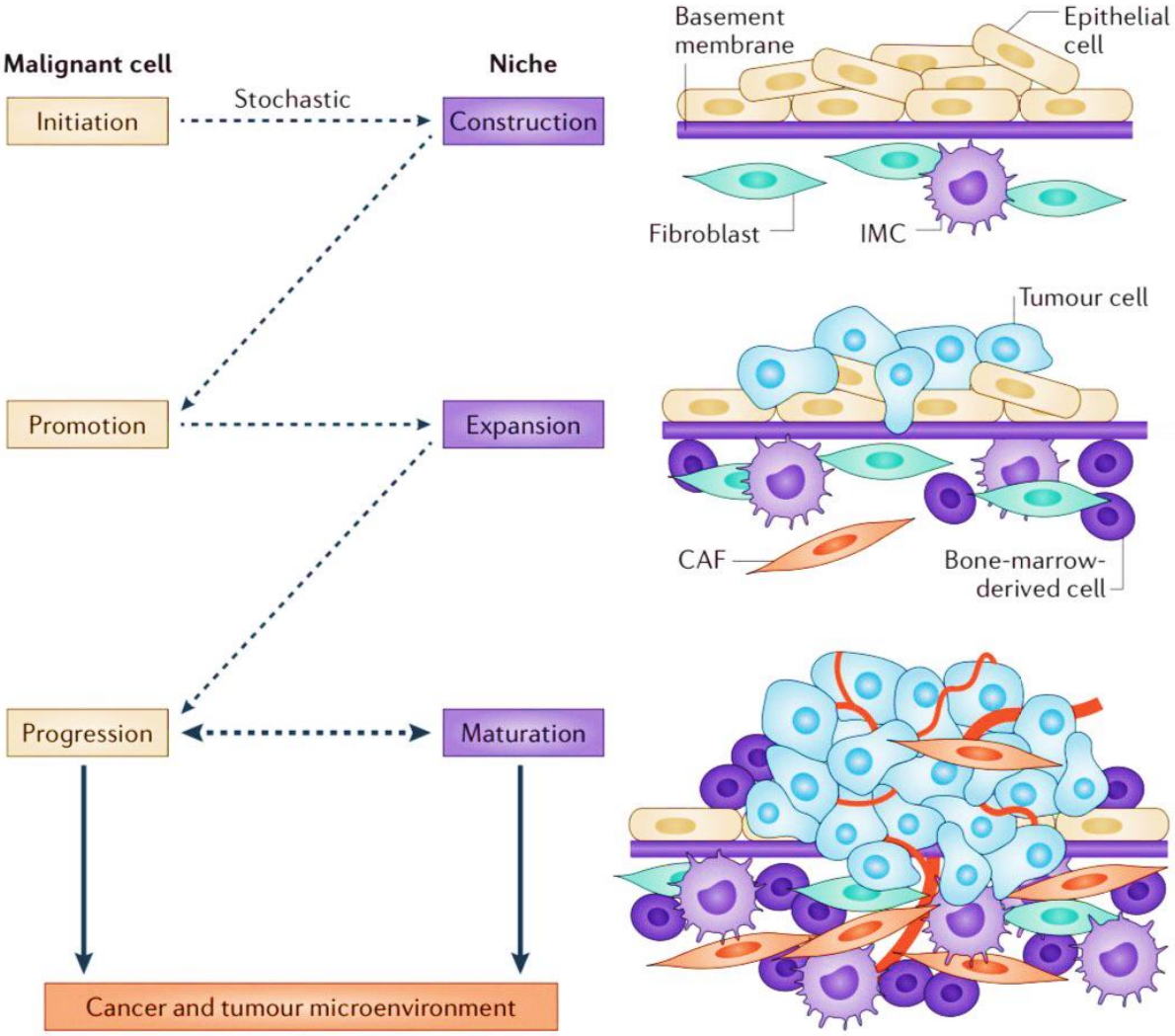

Figure3. Scheme demonstrating metastatic niche formation and maintenance.Tumor initiated cells disrupt the microenvironment's homeostatic features constructing a primary metastatic site. Secreted mediators promote the recruitment of more circulating cells into the metastatic site expanding metastatic growth. Resident cells join the metastatic lesion and induce the formation of new blood vessels (Angiogenesis) to maintain niche maturation.[48]

J. Prostate and Breast cancer

Cancer metastasis develops in 12% of breast cancer patients and account for the majority of cancer-related deaths [84]. For prostate cancer patients, the case is more aggressive where 70% of them develop cancer metastasis[108]. Both breast and prostate metastatic cancer cells follow the parallel progression model during their bone microenvironment invasion [109, 110]. Even with no clear metastatic features, dormant tumor cells colonize secondary sites [111] and non-proliferating DTCs are found in the circulation of 70% of prostate and breast cancer patients [112]. Basically, dissemination features are organs specific. The precise distinct composition of every organ delineates its colonization traits, the kinetic of metastatic infiltration and the aspect of metastatic tropism[113]. Metastatic prostate and breast cancer cells have both a marked predilection to colonize bone marrow niche[114]. The resistance of bone metastasis to anti-tumor treatment increases threat complications [71].

J.1. Prostate cancer cells metastasis to the bone

Metastasis in prostate cancer patients can display either osteoblastic ,osteolytic or mixed lesions [84],but most commonly, patients present with osteoblastic lesions[115]. Tumor cells homing and growth is more preferred in active sites [116, 117]. Since bone microenvironment embodies a plethora of growth factors and cytokines[118], metastatic cancer cells utilize the matrix components to enforce and maintain their survival and proliferation such as TGF-β and MMPs that promote prostate cancer metastasis to bone[119, 120]. Ordinarily, HSCs homing to bone is preserved by bone marrow osteoblasts

and stromal cells with CXCL12 (SDF-1) expression[68]. However, during metastasis, tumor cells compete HSCs for endosteal niche occupancy and osteoblasts adhesion [102]. Moreover, fibroblasts associated to tumor cancer cells; overexpress CXCR4, the complementary receptor of CXCL12, facilitating MSCs recruitment and their trans-differentiation into cancer-mediated fibroblasts. Osteoblasts alignment/arrangement on the bone matrix is altered by their physical contact with prostate metastatic tumor cells [102, 121]. Indeed, osteoblasts microstructure arrangement is modified by tumor-generated pressure[122]. Reaching the secondary tumor site, disseminated prostatic cancer cells activate a variety of intracellular molecular pathways releasing several growth factors such as insulin growth factor-1 (IGF-1), FGF, PDGF, Wnt and endothelin-1 (ET-1), a mitogenic factor inducing osteoblastic differentiation and proliferation [108, 123]. Endothelin-1 is over-expressed in the bone metastatic niche and found to interact with the receptor endothelin A receptor (ETA) [124, 125]. In addition, ET-1 enforces Wnt paracrine signaling pathway by blocking Wnt antagonist dick kopf 1 (DKK1) [126]. Osteoclastogenesis factors secretion is alleviated by the action of urokinase-type plasminogen activator (uPA) [127, 128]. In parallel, osteoclastic activity is blocked due to prostate specific antigen (PSA) release. PSA is a kallikrein serine protease biomarker which plays an essential role in increasing osteoblasts activation and restricting osteoclasts functions by masking PTH-related protein (PTHrP) activity [82].

J.2. Breast cancer cells metastasis to the bone

Breast cancer cells homing to bone cause osteolytic lesions [129] where bone balance is deviated toward osteoclastic hyper activation [130, 131]. Unbalanced

homeostasis stimulates cancer cells to secret TNF-α, IL-11 and PTHrP into the bone microenvironment [71]. Up on this secretion, osteoblasts increase RANKL expression which induces osteoclasts maturation and differentiation [88]. RANKL expression also increases in response to cancer cells secretion of MMPs and their antagonist osteoprotegrin [132, 133]. Bone matrix degradation produces the release of TGF-β which in turn augments the production of PTHrP and IL-11 in the cancer cells and signaling pathways start all over again. This process is called the "vicious cycle" of bone degradation[127] . In addition, TGF-β secretion restricts the immune surveillance and reduces T-cells and NKs function. Intracellular tumor cells auto-phosphorylation, extracellular calcium concentration and mainly IGF-1 maintain the persistence of osteoclastic resorptive "vicious cycle" [134, 135]. TGF-β is also released by the platelets which also engender an osteoclastic activation by platelet-derived LPA (Lysophosphatidic Acid) secretion [136, 137]. In effect, PTHrP is the crucial mediator for osteoclastogenesis in metastatic breast cancer patients. Other factors such as interleukin-1 (IL-1), interleukin-6 (IL-6), interleukin-11 (IL-11), macrophage inflammatory protein 1a (MIP1a), macrophage colony-stimulating factor (M-CSF) and Platelet-derived growth factor (PDGF) are also involved. It has been demonstrated that high levels of IL-1 and IL-6 in the bone metastatic microenvironment boosts the RANKL expression by osteoblasts and other stromal cells and decrease OPG levels promoting osteoclasts differentiation and proliferation. Consequentially, RANKL activates intracellular transcriptional pathways, mainly NF-κB and AP1 (activator protein) and MAPK kinase (mitogen activated protein)[139 ,138 ,93] .

H. Adhesion Mediators

Cell-Cell epithelial interaction is maintained by a variety of intercellular structures such as gap junctions, adherens junctions and tight junctions. Gap junctions retain intercellular communications and cell-cell exchange, although, count for a minor portion of adhesiveness[140]. However, both tight junctions and adherens junctions contribute for the major adhesiveness fraction. Indeed, one of the most dynamic and effective adhesion mediators is cadherin (cadherin-1 or CDH1) [26, 141]. Mutations leading to dysregulation of these mediators provoke tumor cells detachment and enhance loss of epithelial features, thus, strengthen tumor cells migration and dissemination potential. E-cadherin was reported to be lost in cancer cells [141, 142]. In addition, tight junctions delineate the apical pole of epithelial cells. Columnar epithelial cells are held by "gasket-like seals" on their apical region preventing any para-cellular diffusion [143]. Tight junctions involve both integral membrane proteins (occluding, claudin ..) and cytoplasmic proteins (Zonula occludens). ZO proteins associate integral membrane proteins to the actin cytoskeleton filaments [144]. Claudins regulation is an essential mechanism holding EMT during cancer progression [145, 146]. Basically, claudins low expression was reported in both prostate and breast cancer carcinomas [147, 148]. Claudins post-translational modifications including phosphorylation, modifications of molecular pathways such as MAPK pathway [149] as well as phosphatidylinositol 3-kinase (PI3K), clatherin-mediated endocytosis and growth factors affect tight junction's assembly and might interrupt cell-cell contact. In addition, inflammatory mediators like cytokines regulate claudins turnover [150]. For example, interferon (IFN)- γ stimulates

claudin endocytosis and increase tight junctions permeability. Also, TNF-α and IL-13 reduce claudins expression and boost para-cellular permeability [42, 151]. Furthermore, claudin alteration induces claudin co-localization from the membrane to the cytosolic/nuclear compartment in colon cancer patients [152]. Regardless the complexity in the interplay between all the adhesion markers, it is a key to target them for metastatic therapeutic inventions.

H.1. Connexins and Gap Junctions

Connexin family includes twenty members of transmembrane proteins. Each connexin is composed of nine domains: four transmembrane domains and two extracellular loops. Both intracellular loop and C-terminal domain are largely variable between connexin isotypes[154]. Connexin proteins nomenclature is according to their molecular weight[147]. Cx26, Cx30, Cx40, Cx43... are known to maintain different intra and intercellular functions[140]. Energy-consuming, fast connexin turnover rate is 10-25 times greater than other expressed surface proteins. Rapid reaction translates high responding efficacy [153]. The elementary units of gap junctions are connexin proteins. The interaction of two hydrophilic connexons hemi-channel, situated each in a plasma membrane of a cell, forms a gap junction (Figure4). One connexon is a hexagonal assembles of six cylindrical oligomerized protein subunits called connexins[154]. Gap junctions support cell-cell communication and intercellular exchange. Connexin protein is formed of two intracellular domains, two extracellular domains, and four hydrophobic transmembrane domains. These channels are sensitive to calcium concentration, pH, proteins phosphorylation[155]. Connexin43 turn over, assembly, trafficking and channel

gating are regularly governed by several protein interactions[156]. Studies have demonstrated that the inhibition of cadherin function interrupts the formation of gap junctions[148]. Reciprocally, the inhibition of connexin43 disrupts adherens junction formation[157]. Cadherins are transmembrane glycoproteins. They regulate cell adhesion and motility[140]. CTCs dissemination in bone microenvironment is monitored by interactions between E-cadherin (CDH1) of tumor cells - N-cadherin (CDH2) of osteoblasts. In addition, connexin43 interacts with ZO-1[158], the essential component of tight junctions and caveolin-1 in lipid rafts[159]. Trafficking of connexin43 to the plasma membrane is mediated by the formation of the protein complex Cx43-ZO-1-β-catenin.

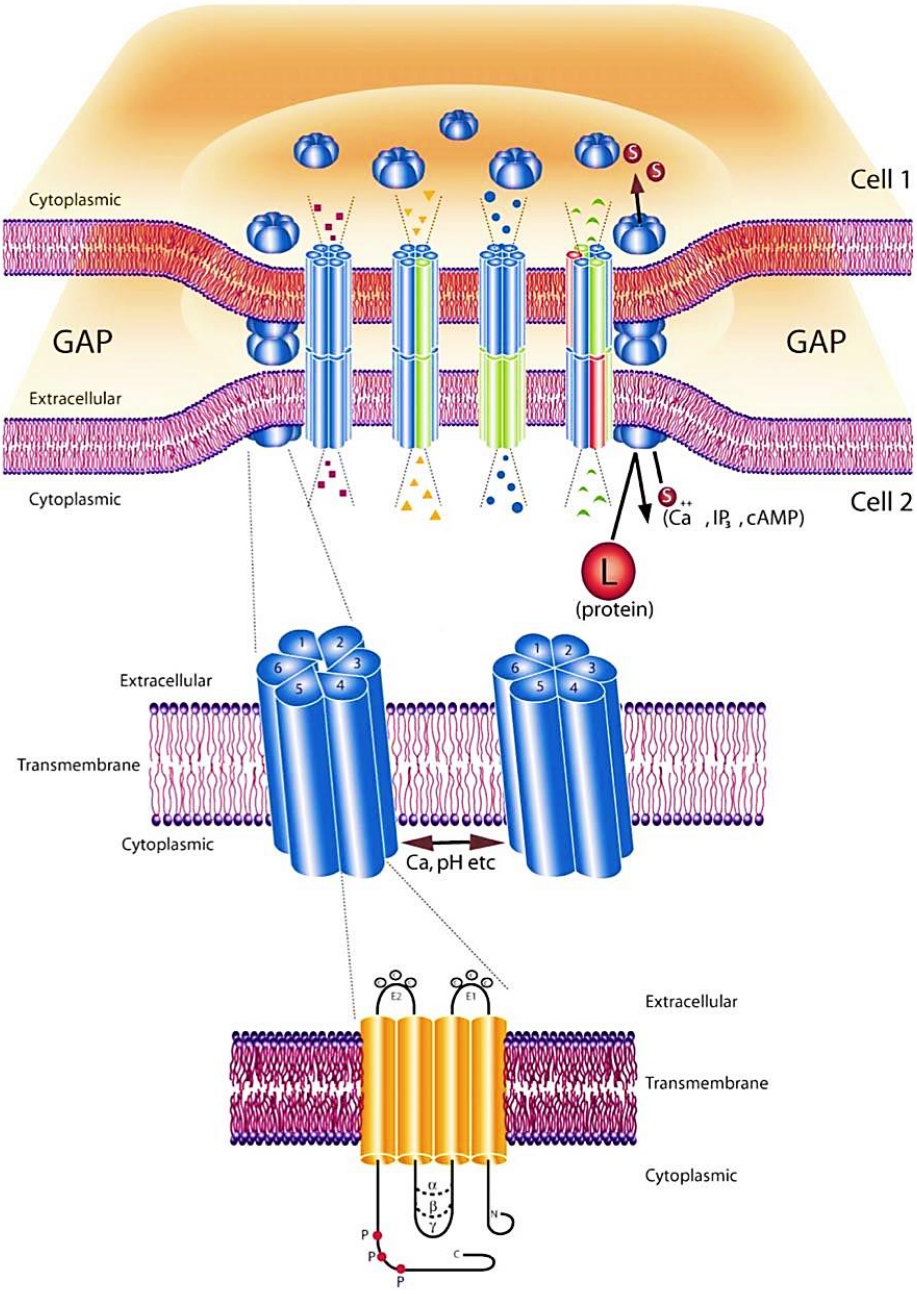

Figure 4. Molecular structure and assembly and of gap junctions. Connexin43 is the elementary unit of a connexon, a hexagonal hemi channel of oligomerized connexin proteins. Gap junctions maintain intercellular communication and molecular exchange. (El-Sabban et al 2003).

H.2. Role of Cx43 in cancer and metastasis

Since tissue homeostasis is maintained by intercellular communications, tumor growth appears to have an effect on gap junction organization and functions. Cx43 is classified as a tumor suppressor protein [160]. Based on previous studies of tumor cells/tissues, Cx43 expression can either increase or decrease based on cancer stage[161].Tightly adherent epithelial cells in the primary tumor site, normally express Cx43 preserving harmony exchange through a process called GJIC (Gap Junction Intercellular Communication) [147]. Primary tumor cells show lower expression of Cx43 due to EMT (Epithelial-to- mesenchymal Transition). The reduction in Cx43 expression is accompanied with down-regulation of epithelial markers such as E-Cadherin and ZO-1 and up-regulation of non-epithelial markers such as N-cadherin [162]. In early stages, Cx43 expression-fluctuations translate a pro-metastatic function [163]. Indeed, tumor cells disengagement from their primary microenvironment is ensured by altering their adhesion with the primary niche.

CTC homing to secondary tumor site is Cx43-dependent. The adhesiveness of CTCs to vascular endothelial cells is a primary process to mediate tumor extravasation [151]. High levels of Cx43 translocate into the apical domain of the endothelial cells to maintain their adhesion to CTCs[164]. Tumor cells extravasate from systemic circulation by para-cellular migration crossing intercellular junctions between adjacent endothelial cells. In addition, extravasation might occur either actively by specific molecules secretion or passively after vessel rupture due to expanding CTCs cellular mass [165]. After crossing the endothelial barrier, DTCs settle in the bone niche. Here, DTCs have

distinctive prospects in binding to mesenchymal stem cells during their differentiation stages ranging from MSCs into osteoblasts via potential adhesion molecules with different adhesion affinities.

CHAPTER II

OBJECTIVE AND AIMS OF THE PROJECT

This study targets prostate and breast cancer cells as a model for malignant solid tumors in humans. The overall aim of this study is to ascertain whether bone metastatic cancer cells adhere to a specific class of cells within bone tissues. We will evaluate adhesion of prostate and breast cancer cells to MSCs and to MSCs induced to differentiate into osteoblastic lineage at different time points by the establishment of an in vitro model of co-cultured: MSC/Osteoblasts - Cancer cells (PC3 as a prostate cancer model and MDA-MB-231 as a breast cancer model). MSCs differentiation, gene expression, cellular localization and protein expression assays will be performed, with the aim of determining the state with the highest cell-cell adhesion affinity and evaluating cancer cells-stem cells to osteoblasts interactions. Thus, exploring specific potential cancer cells molecules involved in initiating and maintaining adhesion to the bones is an essential step to formulate novel modalities for therapeutic intervention.

CHAPTER III

MATERIALS AND METHODS

A. Human cell lines and culture

1. Prostate cancer cells: PC3s

Human mammary epithelial Prostate cancer cells: PC3s are metastatic cancer cells, poorly differentiated human adenocarcinoma. PC3s do not express Protein Specific Antigen (PSA). Cells were sustained in RPMI-1640 medium (Lonza, Walkersville,USA) complemented with 10% of heat-inactivated fetal bovine serum (FBS) (Sigma,St. Louis, USA) and 1% penicillin-streptomycin P/S (Sigma, St. Louis, USA). Media was changed every 48h and cells were passaged every 2 to 3 days. These adherent cells were cultured to 80% confluence in T25 flaks, incubated in a humidified incubator with 95% air and 5% at 37˚C. They were washed with 1x Dulbecco's Phosphate Buffered Saline (PBS), collected by trypsinization by adding 1.5mL of 1x trypsin to the flask and incubate it at 37˚C for 1.5 minutes within the 1x trypsin (Gibco, UK). Collected cells in 1x trypsin were transferred into 15mL flacon tube. The action of trypsin was blocked by adding twice volume of media compared to added volume of 1X trypsin. Collected cells in suspension were centrifuged at 150G for 5 minutes at 22˚C. The supernatant was discarded; the flicked pellet is re-suspended in 3mL of fresh media so can be further seeded for experiments or transferred into T75 flask in a total final volume of 10mL to be later frozen or expanded. Harvested cells were frozen in Cryogenic vials (CORNING® REF: 431386) using 20%FBS, 80%RPMI media and

10% DMSO (Sigma Ref: D2447) in a final number of 1 million cells in a volume of 1mL. Cryovials were placed in a humidified chamber at -80˚C then transferred to liquid nitrogen (-200˚C) for long term storage.

2. Breast cancer cells: MDA-MB-231 (MDA)

Human mammary epithelial Breast cancer cell line: MDA-MB-231 (MDA) established from a pleural effusion. MDA-MB-231 is a hostile, aggressive, poorly differentiated and triple-negative breast cancer cell line. MDAs are characterized by estrogen and progesterone receptors deficiency. Cells were sustained in RPMI-1640 medium (Lonza, Walkersville,USA) complemented with 10% of heat-inactivated fetal bovine serum (FBS) (Sigma,St. Louis, USA) and 1% penicillin-streptomycin P/S (Sigma, St. Louis, USA). Media was changed every 48h and cells were passaged every 2 to 3 days. These adherent cells were cultured to 80% confluence in T25 flaks, incubated in a humidified incubator with 95% air and 5% at 37˚C. They were washed with 1x Dulbecco's Phosphate Buffered Saline (PBS), collected by trypsinization by adding 1.5mL of 1x trypsin to the flask and incubate it at 37˚C for 1.5 minutes within the 1x trypsin (Gibco, UK). Collected cells in 1x trypsin were transferred into 15mL flacon tube. The action of trypsin was blocked by adding twice volume of media compared to added volume of 1X trypsin. Collected cells in suspension were centrifuged at 150G for 5 minutes at 22˚C. The supernatant was discarded; the flicked pellet is re-suspended in 3mL of fresh media so can be further seeded for experiments or transferred into T75 flask in a total final volume of 10mL to be later frozen or expanded. Harvested cells were frozen in Cryogenic vials (CORNING® REF: 431386)

using 20%FBS, 80%RPMI media and 10% DMSO (Sigma Ref: D2447) in a final number of 1 million cells in a volume of 1mL. Cryovials were placed in a humidified chamber at -80˚C then transferred to liquid nitrogen (-200˚C) for long term storage.

3. Bone Marrow Mesenchymal Stem Cells (BMMSC)

Human bone marrow mesenchymal stem cells (MSCs) are progenitor, stromal primary cells distinguished by a high efficiency to differentiate into different cell lines. Cells were maintained in Dulbecco's Modified Eagle Medium-low glucose (DMEM-LG, Sigma Ref: D6046) supplemented with 10% of heat-inactivated fetal bovine serum (FBS) (Sigma,St. Louis, USA) and 1% penicillin-streptomycin P/S (Sigma, St. Louis, USA). Media was changed twice a week and cells were passaged every 2 weeks. These adherent cells were cultured to 80% confluence in T25 flaks, incubated in a humidified incubator with 95% air and 5% at 37˚C. They were washed with 1x Dulbecco's Phosphate Buffered Saline (PBS), collected by trypsinization by adding 1.5mL of 1x trypsin to the flask and incubate it at 37˚C for 1.5 minutes with 1x trypsin (Gibco, UK). Collected cells in 1x trypsin were transferred into 15mL flacon tube. The action of trypsin was blocked by adding twice volume of media compared to added volume of 1X trypsin (Gibco, UK). MSCs are detached from the plastic surface using an additional mechanical force generated by a scraper. Collected cells in suspension were centrifuged at 150G for 5 minutes at 22˚C. The supernatant was discarded; the flicked pellet is re-suspended in 3mL of fresh media so can be further seeded for experiments or transferred into T75 flask in a total final volume of 10mL to be later frozen or expanded. Harvested cells were frozen in Cryogenic vials (CORNING® REF: 431386)

using 20%FBS, 80%RPMI media and 10% DMSO (Sigma Ref: D2447) in a final number of 1 million cells in a volume of 1mL. Cryovials were placed in a humidified chamber at -80˚C then transferred to liquid nitrogen (-200˚C) for long term storage.

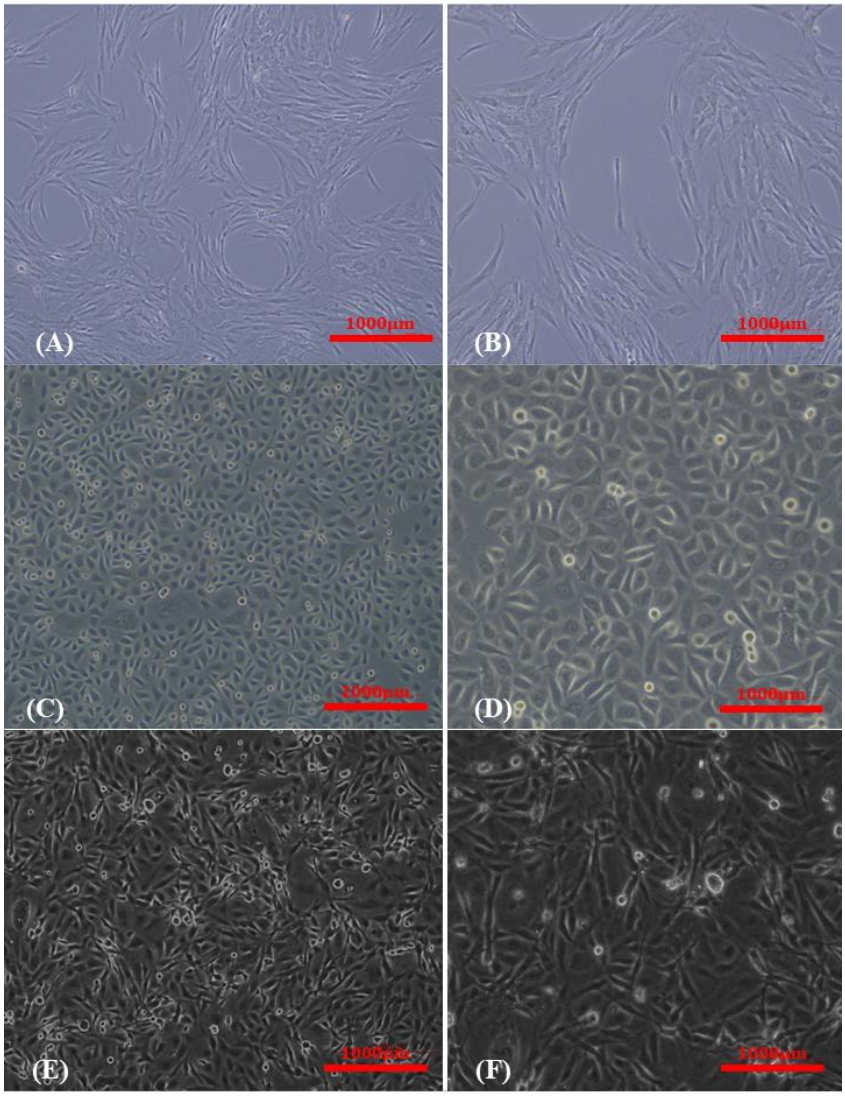

Figure 5. Bright field images of BM-MSCs, PC3s and MDAs. (A; B): Bone marrow-derived spindle-shaped primary MSCs for (A) being at 5x and (B) being at 10x magnifications under light microscope. cultured and maintained in DMEM low glucose medium with a doubling ti me of 2-3 Days. (C; D): Epithelial prostate cancer cells with

an irregular structure for (A) being at 5x and (B) being at 10x magnifications under light microscope. cultured and maintained in RPMI medium. PC3s are fast growing cells with a doubling time of 24-30 hours. (E; F): Spindle shaped epithelial breast cancer cells for (A) being at 5x and (B) being at 10x magnifications under light microscope cultured and maintained in RPMI medium. MDAs are fast growing cells with a doubling time of 30-35 hours.

B. Adhesion Assay

MSCs were seeded in 24 well plate with DAG reefed every 3 days. Series of co-cultures were established at different time points: Day3, 9.12,15,18. At each time point, cancer cells in suspension were added on the top of MSCs in within a fixed co-culture time of 1 hour and fixed ratio of 1/2. After one hour, we aspirated the supernatant and performed trypan blue-based simple count assay. The rest of adherent MSCs-Cancer cells were trypsinized and counted as well. Calculations were percentages-based since the number of differentiated MSCs was gradually increasing with time. The percentage of adhesion was calculated by the number of adherent cancer cells/total number of initially added cancer cells.

C. MSCs : Cancer Cells Co-culture

Direct cell-cell interaction between seeded MSCs and added cancer cells in suspension was established by direct co-culture. MSCs were seeded in 6well-plate. Once reaching 80% confluent, MSCs were refeeded by DAG supplemented low-glucose media every 3 days. Co-culture systems were established at day0 (Before starting DAG) and at Day12. On the co-culture day, media was removed and cancer cells were added in suspension with a ratio of ½. The system was incubated for 30 minutes. Next, media was removed, the system was washed with 1X PBS in order to remive any non-specific

binding. Trypsin 1X was added to the system and incubated for 1minute, than scraped so that MSCs adhered to cancer cells detach from the plastic surface. Harvested cells were transferred to 15mL tube, centrifuged for 5 minutes at 150G and re-suspended in 1X PBS to be further sorted.

D. MSCs differentiation into osteoblasts-like cells Assay

This assay is performed to induce MSCs differentiation into osteoblasts-like cells using DAG. DAG is a mix of three components: Dexamethasone, Ascorbic Acid and β-Glycerophosphate. Dexamethasone stimulates the expression of the osteoblasts differentiation associated transcription factor Runt-related transcription factor 2 (Runx2) by FHL2/β-catenin-mediated transcriptional activation. Ascorbic Acid induces the increase of collagen type I (Col1) secretion which in turn leads to increased Col1/$\alpha_2\beta_1$ integrin-mediated intracellular signaling. β-Glycerophosphate provide needed phosphate for intracellular signaling pathway and bone mineralization. DMEM low glucose media used to re-feed mesenchymal stem cells three times per week.

E. Calcium deposit Assay

Alizarin Red stain is used to identify calcium deposits in osteoblasts like-cells differentiated from mesenchymal stem cells. Seeded MSCs were washed twice with 1X PBS, fixed with 4% PFA for 30 minutes, washed with distilled water, incubated in Alizarin Red for 30 minutes at room temperature, washed by distilled water, and finally the plate is left to dry. Pictures are taken using light microscope.

F. Fluorescence- Activated Cell Sorting (FACS)

Fluorescent cells were isolated using a BD FACS Aria SORP cell sorter in the single cell mode at a low sort rate. Co-cultured MSCs and cancer cells to be sorted were trypsinized, scraped, and pooled together. The action of 1X TE was blocked by adding media. Cell suspension was centrifuged at 150G for 5 minutes. The pellet was then washed with 1X PBS. Cells were sorted based on their difference in size (MSCs: large cells and PC3s/MDAs: Small cells), there was no need for a marker and no need for a negative control. Taken in collection tubes filled with corresponding media for each cell line, the suspension was first centrifuged, washed with PBS and then centrifuged again. Proteins and RNA were extracted from the pellet.

G. RNA extraction, cDNA Synthesis and Quantitative Real-Time PCR (qRT-PCR)

1. RNA Extraction

Total RNA was extracted using QIAGEN RNeasy Kit (Quiagen ®Reference: 74134) according to manufacturer's instructions. The first step is cell lysis by adding Buffer RLT containing β-Mercaptoethanol. RLT lysis buffer deactivates RNases allowing appropriate absorption of RNA to the silica membrane. During the preparation, DNase solution is directly applied to the silica membrane in order to remove genomic DNA. Several washes are performed. Final pure RNA is eluted in 30µL RNase free water.

RNA concentration was measured using NanoDrop spectrophotometry. RNA purity was assessed by the absorbance ratio 260nm/280nm with a value of 1.8-2 indicating pure RNA.

2. cDNA Synthesis

Using BIO-RAD cDNA synthesis Kit, 1 µg of total extracted RNA was reversed transcribed to cDNA. Real-time PCR was performed using iQ SYBR Green Supermix in a CFX96 system (Bio-Rad Laboratories). The 5x iScript Reaction Mix contains primers, nucleotides for DNA synthesis (dNTPs), MgC2 and buffers required by the enzymes. The complete reaction mix is incubated in a thermal cycler, priming for 5 minutes at 25˚C, followed by reverse transcription (RT) for 20 minutes at 46˚C and RT inactivation for 1 minute at 95˚C.

3. *Real Time PCR (qPCR)*

Using 1µg of single strand cDNA mixed with 10µL SyberGreen (Green fluorescent cyanine dye with high sffinity for double-stranded DNA). The mix was loaded in duplicates with forward and reverse specific primers for every gene in CFX96 system (Bio-Rad). Used primers for this project are able to recognize Cx43, ALP, N-Cad, E-Cad, and the Housekeeping gene GAPDH listed in table 1.

Real-Time PCR Steps are as following: precycle of 95˚C for 3 min followed by 40 cycles consisting of 95˚C for 10 sec, X˚C for 30 sec and 72˚C for 30 sec and a final extension step at 72˚C for 5 min. DNA amplification is obtained for each gene as "Fluorescence Threshold Cycle Value Ct", comparative cycle threshold (ΔΔCT) which

will be used to describe the relative-fold variation in the expression of each gene normalized to GAPDH expression.

Table 1: Human real-time primers with their relative sequences and annealing temperatures

(F= Forward primer R= Reverse primer).

Genes	**Primers' Sequences**	**Annealing Temperature (˚C)**
Cx43	F: CTTCACTACTTTTAAGCAAAAGAG R: TCCCTCCAGCAGTTGAG	52
ALP	F: ACAAGCACTCCCACTTCATCTGGA R: TCACGTTGTTCCTGTTCAGCTCGT	58
N-Cad	F: GGTGGAGGAGAAGAAGACCAG R: GGCATCAGGCTCCACAGT	58
E-Cad	F: CAGAAAGTTTTCCACCAAAG R: AAATGTGAGCAATTCTGCTT	58
GAPDH	F: TGGTGCTCAGTGTAGCCCAG R: GGACCTGACCTGCCGTCTAG	52 – 62

H. Protein Extraction and Immunoblot

1. Cellular Protein Extraction

In order to be able to study the protein expression by Western Blot Analysis, lysing cells is the first step for cell fractionation, organelles isolation and protein extraction. Cells were seeded in 6 well-plate, co-cultured, sorted than centrifuged. The extraction was performed from the obtained pellet. Approximately 20µL of Lysis buffer (0.125 M Tris-HCl (pH 6.8), 2% sodium dodecyl sulfate (SDS) and 10% glycerol) supplemented with 20 µl/ml protease inhibitors and 100 µl/ml phosphatase inhibitors were added per well on cells which were scraped.

For protein quantification, DC Protein Assay (Bio-Rad, Hercules, CA) was used based on establishing a standard curve of bovine serum albumin (BSA, Sigma Chemical Co.) using ELISA Reader to determine the concentrations.

2. Western Blot Analysis

To examine the levels of proteins expression, Western Blot was performed. Protein samples were prepared by adding a correspondent volume to 100 µg of extracted proteins, equal volume of 2x Sample Buffer (50mM Tris-HCl; pH=6.8, 2%SDS, 10%Glycerol), and 5% β-Mercaptoethanol. Hydrogen bones were broken by heating, where samples were kept for 10minutes at 95˚C. Samples were then loaded and resolved on 8% SDS-PAGE gels at 30mA. The gel's concentration is based on the molecular weight of target proteins. Ladder (Molecular weight standard) was also added

in a separate well. After electrophoresis separation, proteins were electrically stimulated overnight at 30V to be transferred on PVDF membranes (Bio-Rad Laboratories) using a cassette. After transfer, the membrane was blocked by 5% skimmed milk, and then incubated with specific primary (Table2). The blot was washed with 1x PBS and then incubated with the secondary specific antibodies at room temperature (Santa Cruz Biotechnology, Santa Cruz, CA). The membrane was washed again, chemiluminescent substrate was applied and band were visualized using ChemiDoc (MP imaging System Biorad). Equivalent loading was ascertained by GAPDH probing.

Table2: List of primary antibodies recognizing human antigen

Primary Antibody	Source	Used Concentration
Cx43	Sigma	1 µg/mL
N-Cad	ThemroFisher	1 µg/mL
GAPDH	Abnova	1 µg/mL

I. Immunofluorescence (IF) and confocal microscopy

Immunofluorescence (IF) was performed on MSCs co-cultured with cancer cells seeded on glass coverslips. Cells were incubated for 30minutes to allow the interaction between MSCs and cancer cells. The co-culture system was fixed with 100% Ethanol and then washed twice with PBS 1X, then blocked with 3% BSA for 1 hour in humidified chamber. Cover slips were then incubated with Cx43 and N-Cad primary antibodies overnight. Next day, cover slips were washed twice with PBS 1X, incubated

with the corresponding fluorescent secondary antibody for 1 hour, and then with DAPI for 10 minutes to stain their nuclei with consequential PBS 1X washes. Cover slips are finally mounted on slides using Prolong Anti-fade kit and stored at 4˚C in the dark.

Confocal images were obtained with a laser scanning confocal microscope (LSM 710, Zeiss, Germany) using x20 and x63 oil objectives. Slides were sequentially excited by laser at different wavelengths. Images were analyzed by Zeiss Zen 200g microscope software.

CHAPTER IV

RESULTS

A. Assessment of the maximum adhesion state

In vitro, DAG is used to stimulate MSCs differentiation into osteoblasts-like cells during 21 days. Since the overall aim of this project is to ascertain whether bone metastatic cancer cells adhere to a specific class of cells within the bone tissue, we trapped the percentage of MSCs/PC3s adhesion at different time points: 5, 8,10,12,15 and 18 along with MSCs differentiation. Seeded MSCs were refeeded by DAG every 2 days. At each time point, we co-cultured MSCs with PC3 in a ½ ratio for 1 hour.

As shown in Figure8, the established adhesion graph revealed a graduate increase of MSCs to PC3s adhesion percentage, reaching a maximum of 88% at day 12. Hence, day12 will be our target in studying in depth the molecular and cellular variations up on their co-culture with cancer cells.

Adhesion percentage is calculated by simple count based on the number of remaining non-adherent PC3s in the supernatant at each time point after 1 hours of co-culture with a constant PC3s to MSCs ratio.

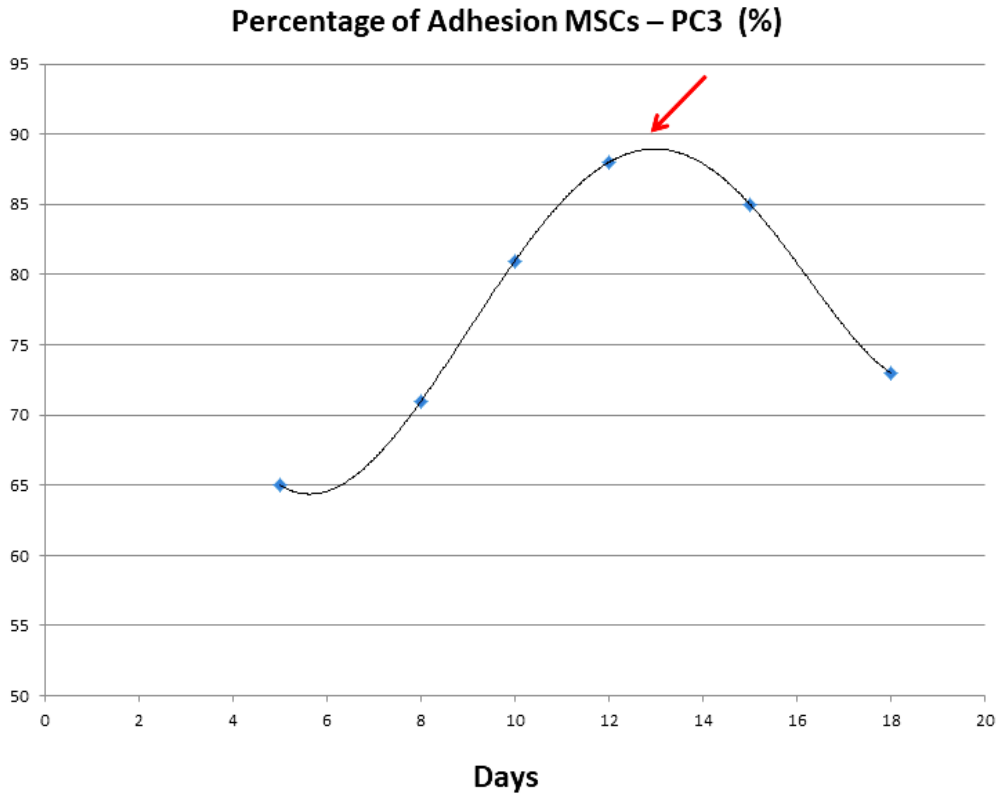

Figure 6. Assessment of the percentage of adhesion of MSCs to PC3s at different time points: day5, 8,10,12,15 and 18 by the establishment of co-culture system adding PC3s in suspension on the seeded MSCs with a ratio of ½, for 1hour. The percentage of adhesion was seen on day12, where 88% of PC3s adhered to seeded partially differentiated MSCs.

B. Time and Ratio Course

Knowing that day12 displayed the maximum adhesion of induced-differentiation MSCs into osteoblastic lineage to cancer cells, we wanted to know the optimal time and ratio in MSCs/cancer cells co-culture. For this reason, serial co-cultures were performed at different MSCs to cancer cells times and ratios. Adhesion percentages were then calculated and assembled as shown in the Figure 9.

For both cancer cell lines, adhesion percentage increases proportionally to cancer cells ratios; all of these percentages end up reaching a “plateau”, within this stage, all cancer cells are forced to adhere. Hence, the optimal co-culture time, is the time point just before reaching the “plateau” so that cancer cells are not forced to adhere, behaving spontaneously, and being studied as close as possible to their physiological normal conditions.

Using light microscopy, we assessed the optimal ratio of MSCs to cancer cells. The best adhesion ration is ½ where cells are not as few as ¼ ratio, neither as numerous as 1/1 ratio.

This graph also reflects considerable difference in adhesion percentage between both prostate and cancer cells. The highest adhesion plateau of PC3 is approximately 50%, higher than the MDAs maximum reached plateau which is 43%. PC3s show 20% more adhesion to MSCs than MDAs.

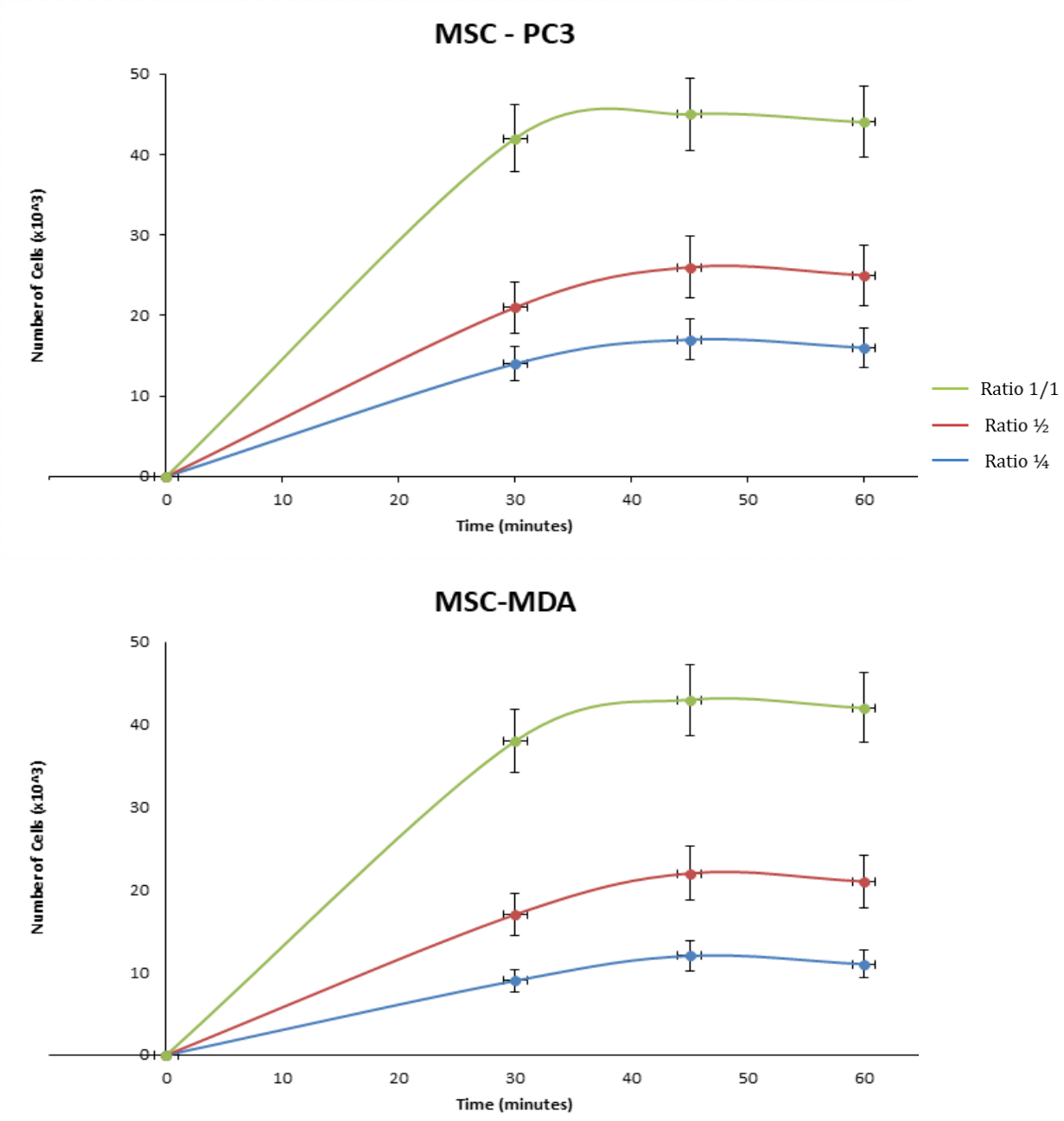

Figure 7. The percentage of adhesion of MSCs to cancer cells (PC3 and MDA) along with a time and ratio course. The percentage of adhesion increases proportionally with the ratio of added cancer cells. The percentage of adhesion ends up reaching a plateau where all cancer cells are forced to adhere. The best time for the establishment of the co-culture is 30 minutes the time just before reaching the plateau where cancer cells adhere spontaneously. The best ratio of MSCs/cancer cells is ½ assessed by light microscope.

C. Assessment of MSCs differentiation into osteoblasts-like cells Assay via light microscopy

DAG shifts the intracellular signaling cascades in marrow stroma-derived stem cells leading to osteogenic differentiation.

DAG efficiency in stimulating and maintaining MSCs differentiation into osteoblasts can be assessed by trapping MSCs morphological changes under the microscope.

Up on adding DAG to MSCs medium, their spindle shape switches gradually to cuboidal/round shape as shown in Figure10.

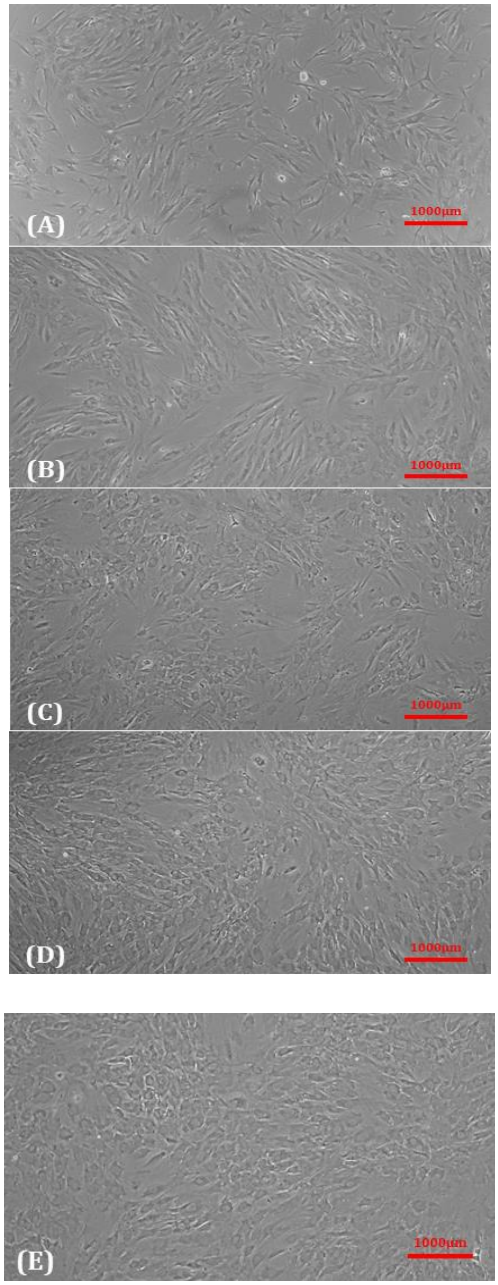

Figure 8. MSCs Morphological Changes at microscopic levels up on DAG refeed. Up on DAG refeed, MSCs, trapped at different time points, lose gradually their spindle shape and gain a round, osteoblast-like shape. (A): MSCs without DAG _ Day0, (B): MSCs + DAG _ Day3, (C): MSCs + DAG _ Day6, (D): MSCs + DAG _ Day9, (E): MSCs + DAG _ Day12.

D. Assessment of MSCs differentiation into osteoblasts-like cells Assay via Alizarin Red Assay

To further ascertain MSCs differentiation into osteoblasts-like cells, we stained differentiated MSCs with alizarin red which is a common stain used to detect and identify differentiated MSCs calcium content. The end product alizarin Red S-calcium complex in a chelation process is bright red stain.

Day0 MSCs display no calcium deposits. Same lack of red staining is observed in confluent MSCs at day12 non-treated with DAG. However, MSCs treated with DAG, at day12 showed red plaques of calcium deposits which are marker of their differentiation into osteoblasts-like cells, as shown in Figure9.

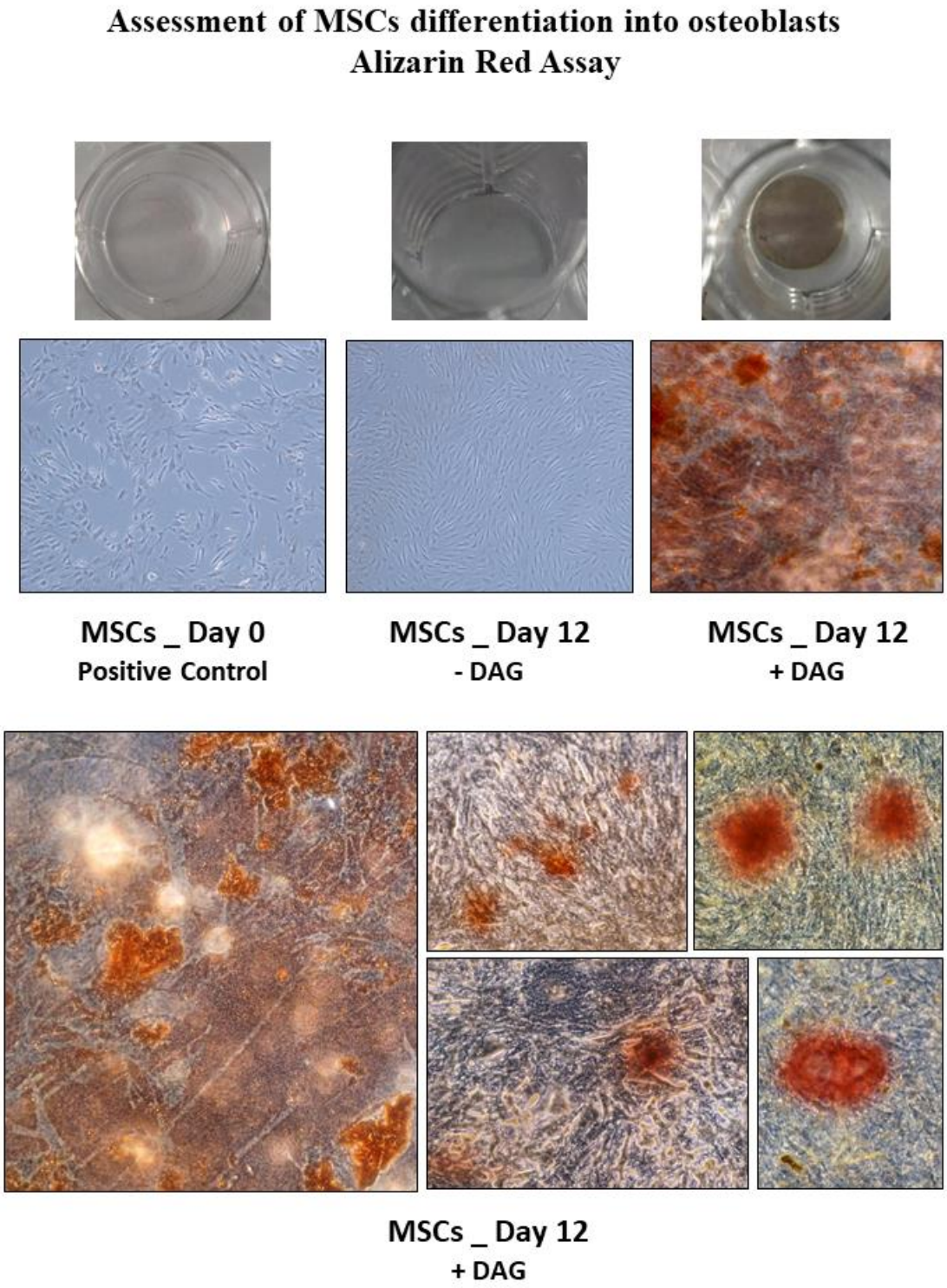

Figure 9. Alizarin red images taken for wells with light microscopy showed red calcium deposits as a marker of MSCs differentiation into osteoblasts-like cells. No red staining at both day0 and day12 without DAG refeed.

E. Assessment of MSCs differentiation into osteoblasts-like cells Assay via qRT-PCR analysis

ALP is an enzyme with catalytic function mostly found in bone cells. Along with their differentiation into osteoblasts like cells, MSCs express ALP gradually. For this reason, qRT-PCR was performed for each set of MSCs at day 0 and 12 (in parallel with performing DAG).

As shown in Figure10-A, significant increase of ALP expression at day 12 in MSCs to be cultured with PC3s is detected by approximately 4 folds with P_{value} = 0.0005.

As shown in Figure10-B, significant increase of ALP expression at day 12 in MSCs to be cultured with PC3s is detected by approximately 5 folds with P_{value} = 0.0021.

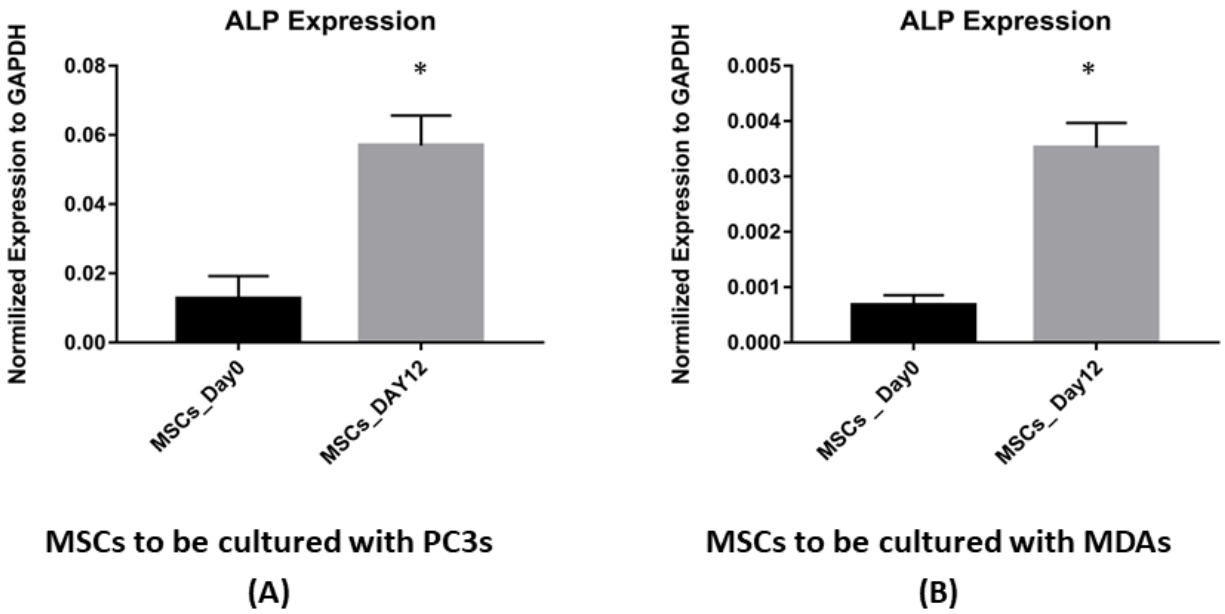

Figure 10. Graphical representation of changes in mRNA expression levels of ALP gene normalized to GAPDH housekeeping gene in MSCs at day 0 and 12 up on DAG reefed. ALP expression increases up on DAG refeed.

F. Co-culture Images

Once MSCs are 80% confluent, Day0 co-culture was performed for 30 minutes with a ½ ratio of MSCs/PC3s. On the same day, we started DAG refeed for another set of MSCs to stimulate MSCs differentiation into osteoblast-like cells which were co-cultured with cancer cells after 12 Days.

By comparing light microscopy images after co-culture of each cancer cell line, we can detect higher scale of PC3s adherence to MSCs at day12 as shown in Figure12 (B) compared to MDAs adherence as shown in Figure 14(B).

1. MSCs/PC3s Co-culture

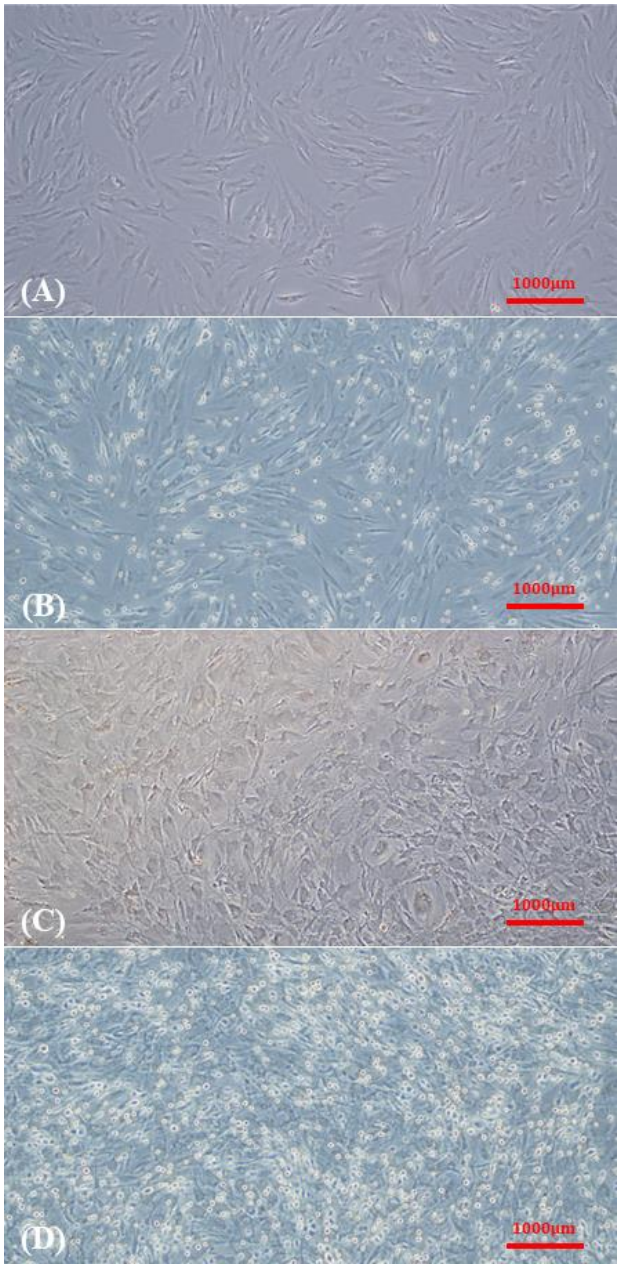

Figure 11. Bright field images of MSCs before and after co-culture with PC3 cells at day0 and day12. (A): Non-differentiated MSCs at day0 before co-culture with PC3s, (B): Non-differentiated MSCs at day0 in PBS 1X after removing medium containing the non-adherent PC3s.(C): Differentiated MSCs by DAG at day12 before co-culture with PC3s. (D): Differentiated MSCs by DAG at day12 in PBS 1X after removing medium containing the non-adherent PC3s.

2. MSCs/MDAs Co-culture

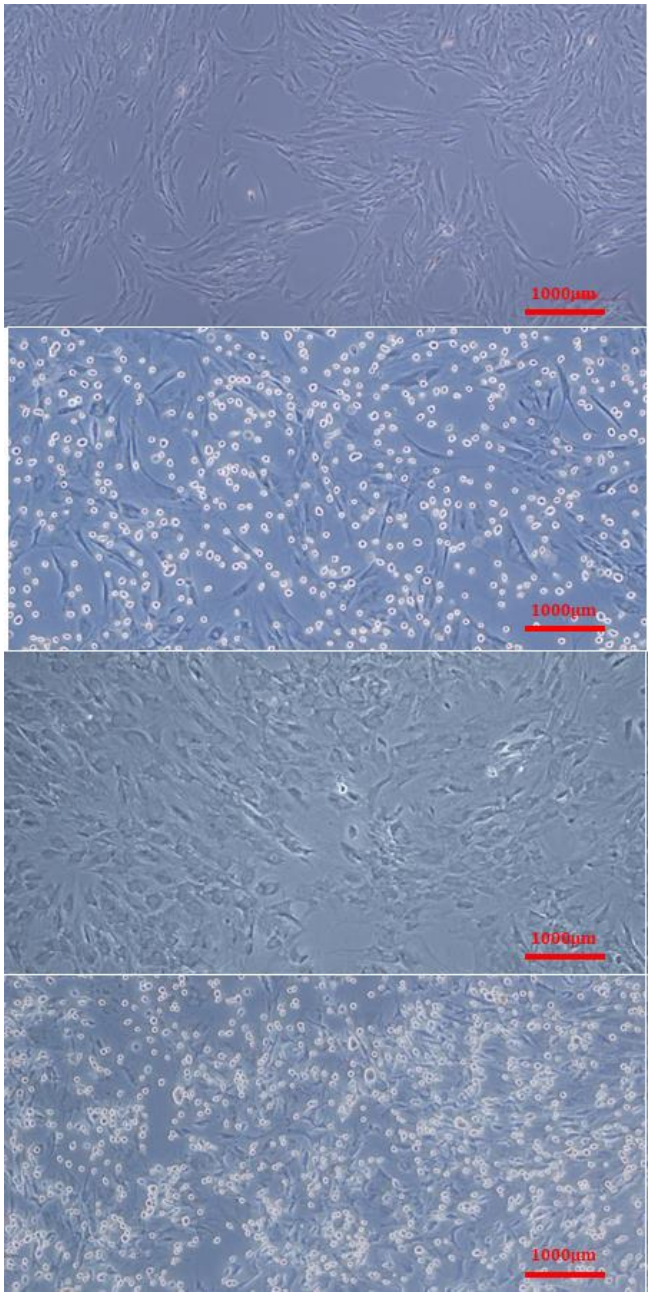

Figure 12. Bright field images of MSCs before and after co-culture with MDAs cells at day0 and day12. (A): Non-differentiated MSCs at day0 before co-culture with MDAs, (B): Non-differentiated MSCs at day0 in PBS 1X after removing medium containing the non-adherent MDAs.(C): Differentiated MSCs by DAG at day12 before co-culture with MDAs. (D): Differentiated MSCs by DAG at day12 in PBS 1X after removing medium containing the non-adherent MDAs.

G. Sorting Data

After being co-cultured with cancer cells, MSCs-Cancer cells were trypsinized, scraped it and re-suspended it in PBS 1X. Harvested cells were sorted based on their difference in size. The size and granularity of MSCs at each passage were also evaluated using the flow cytometry forward and side scatter diagram. Sorting data revealed 2 distinguished populations. The large-sized cells: MSCs (population in pink) and the small-sized cells: PC3s and MDAs (population in blue) as shown in Figure17 and 18.

At both days the percentage of adhesion of cancer cells to MSCs increases at day12 compared to day0.

The percentage of adhesion of MSCs to PC3s increases with an 18.2% between day0 and 12. However, the percentage of adhesion of MSCs to MDAs increases with a 2.2% between day0 and 12. Differential increase reflects higher potential of PC3s adhesion to differentiated MSCs at day12 compared to MDAs.

1. MSCs/PC3s

As shown in Figure17, day0 showed two distinct populations of MSC (large size cells) and PC3 (small size cells) with 770/4277 adhesion percentage which is equivalent to 18%. This percentage increases significantly at day12 with 1457/4025 adhesion percentage which is equivalent to 36.20%.

Differentiated MSCs-PC3s adhesion affinity increases at day12 compared to day0 which confirms previous culture work.

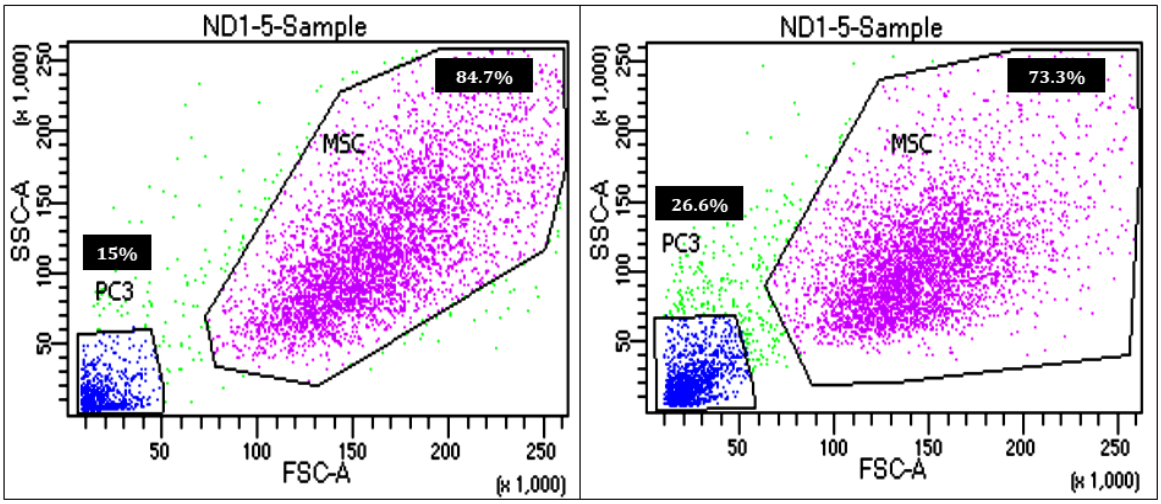

Figure 13. Size-based sorting-data_MSCs/PC3s showed 2 populations; one with small size representing PC3s population, and another with large size representing MSCs population. The percentage of adhesion is calculated by the ratio of the fraction of each population on the total number of cells. Day12 showed higher percentage of adhered PC3s to partially differentiated MSCs compared to undifferentiated MSCs at day0.

2. MSCs/MDAs

Day0 showed two distinct populations of MSC (large size cells) and MDA (small size cells) with 722/5082 adhesion percentage which is equivalent to 14.2%. This percentage increases significantly at day12 with 898/5588 adhesion percentage which is equivalent to 16.4%.

MSC-PC3 adhesion affinity increases slightly on day12 compared to day0 which confirms previous culture work.

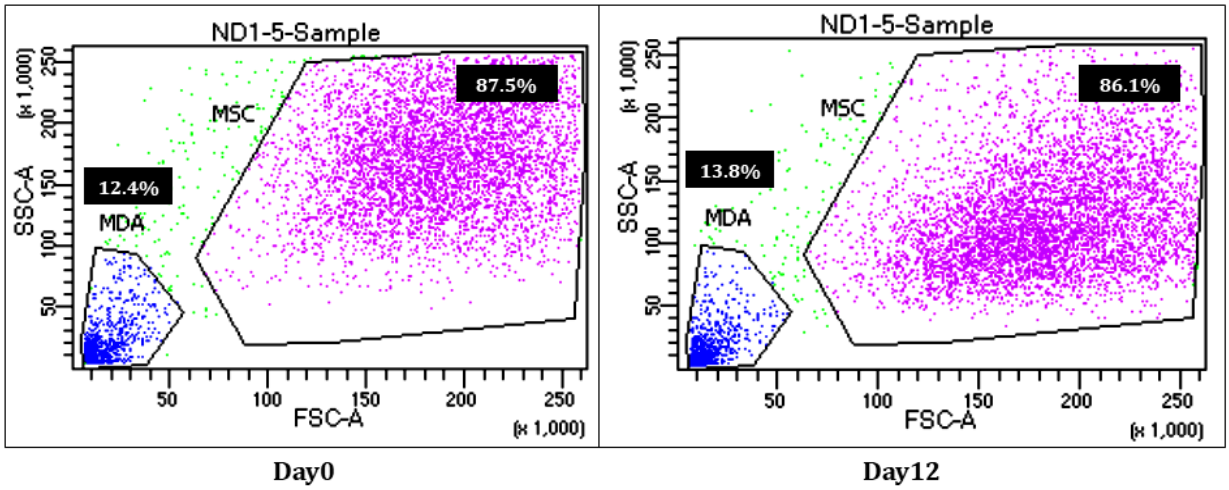

Day0 **Day12**

Figure 14. Size-based sorting-data_MSCs/MDAs showed 2 populations; one with small size representing MDAs population, and another with large size representing MSCs population. The percentage of adhesion is calculated by the ratio of the fraction of each population on the total number of cells. Day12 showed higher percentage of adhered MDAs to partially differentiated MSCs compared to undifferentiated MSCs at day0.

H. Assessemnet of Cx43 Expression

The elementary proteins of gap junctions, cx43 are involved in maintaining cell-cell interactions. Hence, might be playing a key role in maintaining MSCs to cancer cells adhesion.

1. Decrease of Cx43 Expression in MSCs co-cultured with PC3s

In order to evaluate molecular vaiations in MSCs co-cultured with PC3s, cx43 expression at the genetic and protein level, we performed qRT-PCR, Western Blot analysis and immunofluorescnce assyas on sorted MSCs before and after co-culture at day0 and day12.

Cx43 expression in sorted MSCS decreases up on co-culture at day0 by approximately 2 folds as shown in Figure15-A-1. Similarly, cx43 expression in sorted

MSCs decreases up on co-culture at day12 by approximately 2.5 folds as shown in Figure19-A-2.

The decrease at day12 with $P_{value} = 0.0148$ is more significant than day0 with $P_{value} = 0.0870$.

This was also confirmed by western blot analysis, as shown in Figure15-B, cx43 protein expression decreases at both day0 and 12 up on co-culture, but more significantly at day12. An additional band with a molecular weight of 57 KDa is also detected at day0 and day12 after co-culture.

Immunofluorescence images reflect a decrease in cx43 expression in MSCs up on co-culture with PC3s at day0 and day12. Decrease in cx43 expression is more significant up on co-culture at day12 compared to day0 as shown in Figures 16 and 17. At the morphological level, we can clearly distinguish a switch in the spindle shape of MSCs toward round-shaped morphology post co-culture.

In addition, at day 12 we detected a clear loss of spindle shape MSCs, this is due to DAG assay, ensuring a partial differentiation of MSCs into osteoblasts-like cells during 12 days ((as indicated by arrows).

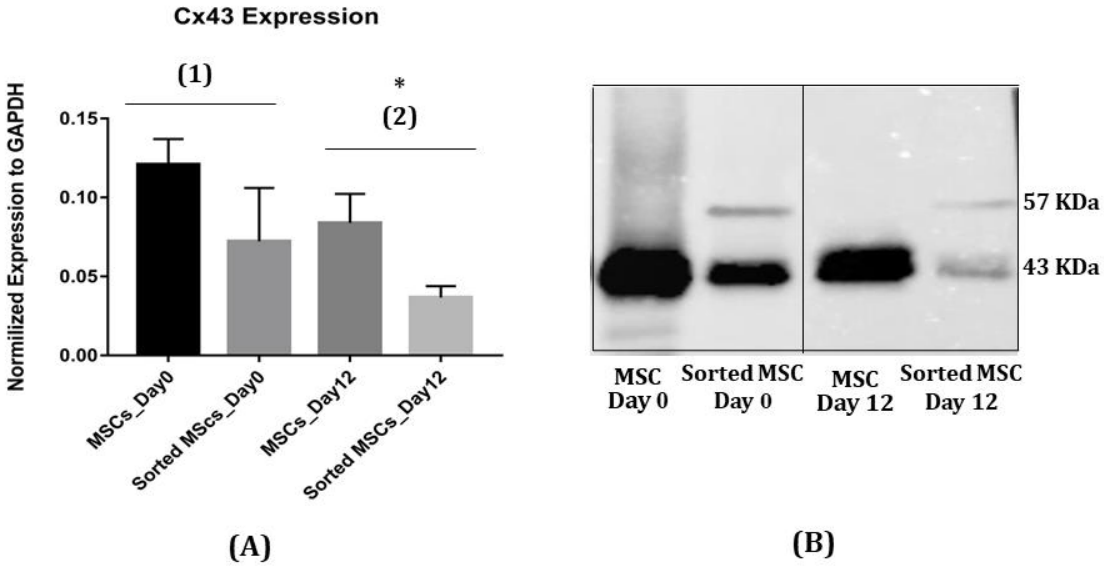

Figure 15. Gene and protein expression of Cx43 in sorted mesenchymal stem cells co-cultered with PC3s. (A): Graphical representation of changes in mRNA expression level normalized to GAPDH housekeeping gene showed a decrease in the expression of cx43 in MSCs up on co-culture with PC3s in both time points: day 0 and 12. (A1): 41.11% decrease in cx43 expression up on co-culture of MSCs with PC3s at day0, (A2): 56.16% decrease in cx43 expression up on co-culture of MSCs with PC3s at day12. (B): Western blot analysis showed similarly a much more considerable decrease in cx43 expression on day12 than day0.

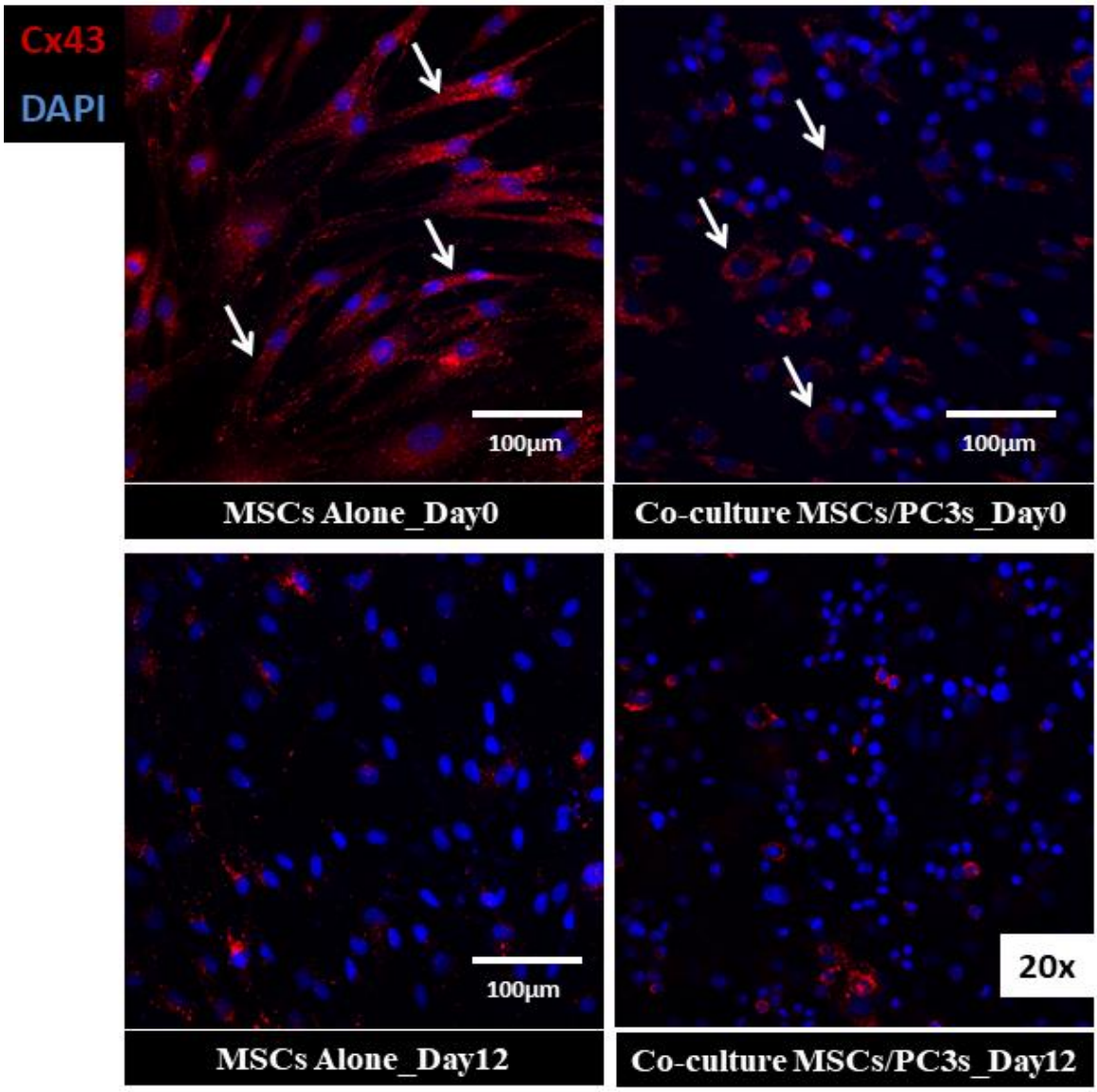

Figure 16. Immunofluorescence images of mesenchymal stem cells co-cultered with PC3s (20x). Images showed a decrease in the expression of cx43 in MSCs post-co-culture with PC3s at both day0 and day12. Cx43 decrease is much more significant at day12. White arrows indicate the morphological changes of MSCs up on co-culture with PC3s. MSCs alone showed a spindle shaped structure, which switches into irregular structure after co-culture.

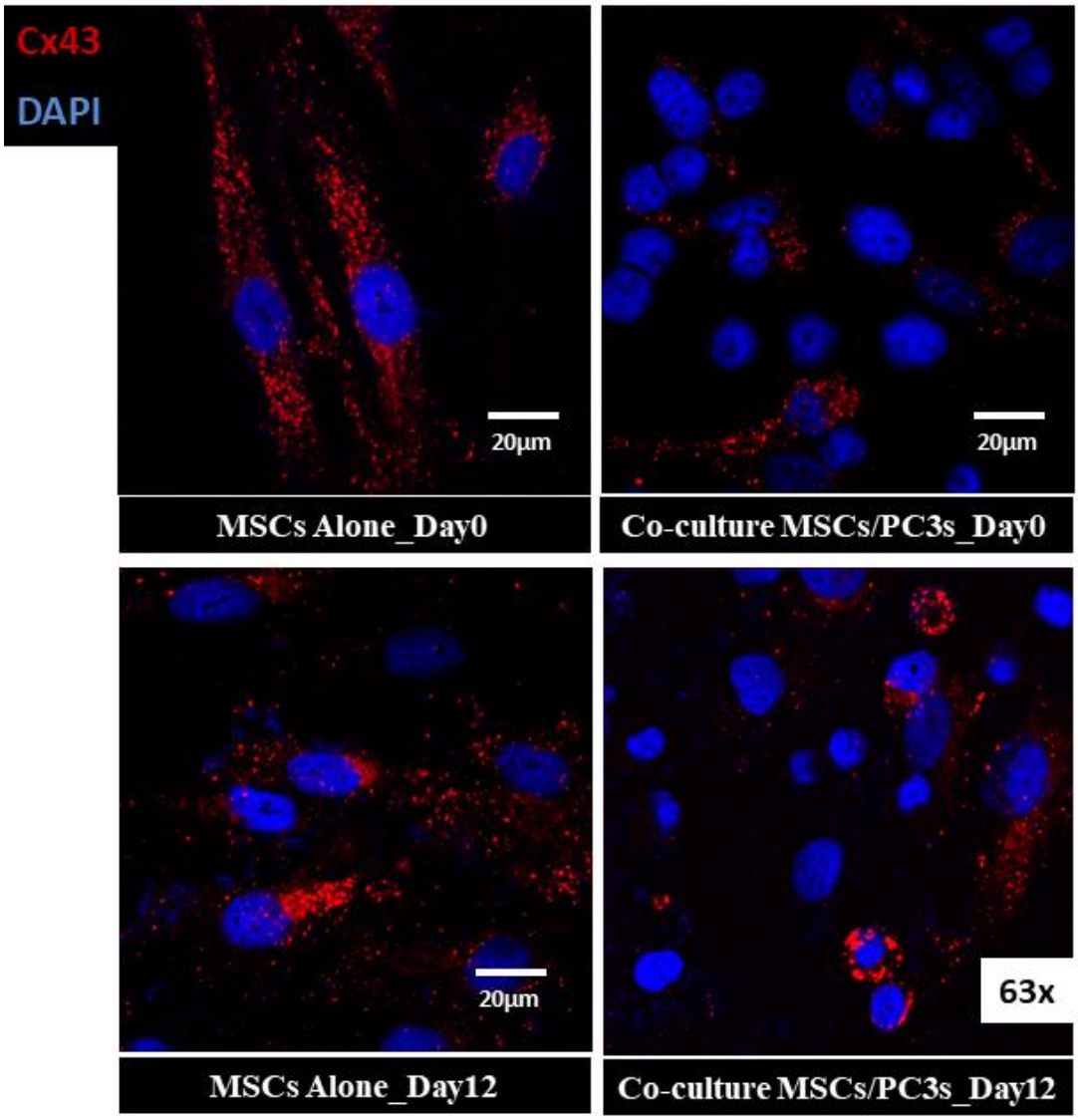

Figure 17. Immunofluorescence images of mesenchymal stem cells co-cultered with PC3s (63x,Oil). Images showed a decrease in the expression of cx43 in MSCs post-co-culture with PC3s at both day0 and day12. Cx43 decrease is much more significant at day12.

2. Decrease of Cx43 Expression in MSCs co-cultured with MDAs

In order to evaluate molecular vaiations in MSCs co-cultured with MDAs, cx43 expression at the genetic and protein level, we performed qRT-PCR, Western Blot

analysis and immunofluorescnce assyas on sorted MSCs before and after co-culture at day0 and day12.

Cx43 expression in sorted MSCS decreases up on co-culture at day0 by approximately 1.5 folds as shown in Figure18-A-1. Similarly, cx43 expression in sorted MSCs decreases up on co-culture at day12 by approximately 2 folds as shown in Figure18-A-2.

The decrease on day12 with $P_{value} = 0.0017$ is more significant than day0 with $P_{value} = 0.0419$.

This was also confirmed by western blot analysis, as shown in Figure18-B, cx43 protein expression decreases at both day0 and 12 up on co-culture, but more significantly at day12. An additional band with a molecular weight of 57 KDa is also detected at day0 and day12 after co-culture.

Immunofluorescence images reflect a decrease in cx43 expression in MSCs up on co-culture with MDAs at day0 and day12. Decrease in cx43 expression is more significant up on co-culture at day12 compared to day0 as shown in Figures 19 and 20. At the morphological level, we can clearly distinguish a switch in the spindle shape of MSCs toward round-shaped morphology post co-culture.

In addition, at day 12 we detected a clear loss of spindle shape MSCs, this is due to DAG assay, ensuring a partial differentiation of MSCs into osteoblasts-like cells during 12 days (as indicated by arrows).

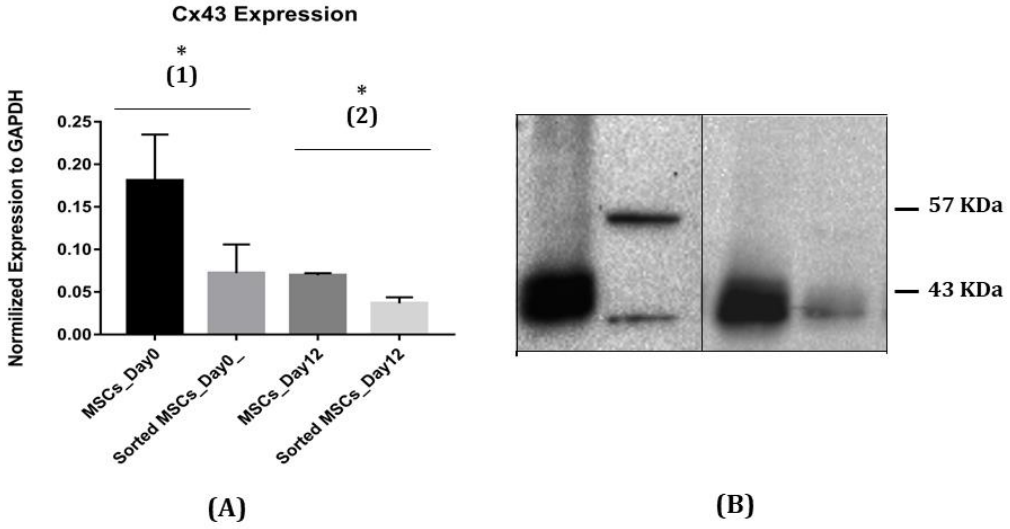

Figure 18. Gene and protein expression of Cx43 in sorted mesenchymal stem cells co-cultered with MDAs.(A): Graphical representation of changes in mRNA expression level normalized to GAPDH housekeeping gene showed a decrease in the expression of cx43 in MSCs up on co-culture with MDAs in both time points: day 0 and 12. (A1): 13.11% decrease in cx43 expression up on co-culture of MSCs with MDAs at day0, (A2): 21.59% decrease in cx43 expression up on co-culture of MSCs with MDAs at day12. (B): Western blot analysis showed similarly a much more considerable decrease in cx43 expression on day12 than day0. An extra band was detected in western blot on day12 with a molecular weight of 57KDa. This might be due to cx43 post translational modifications.

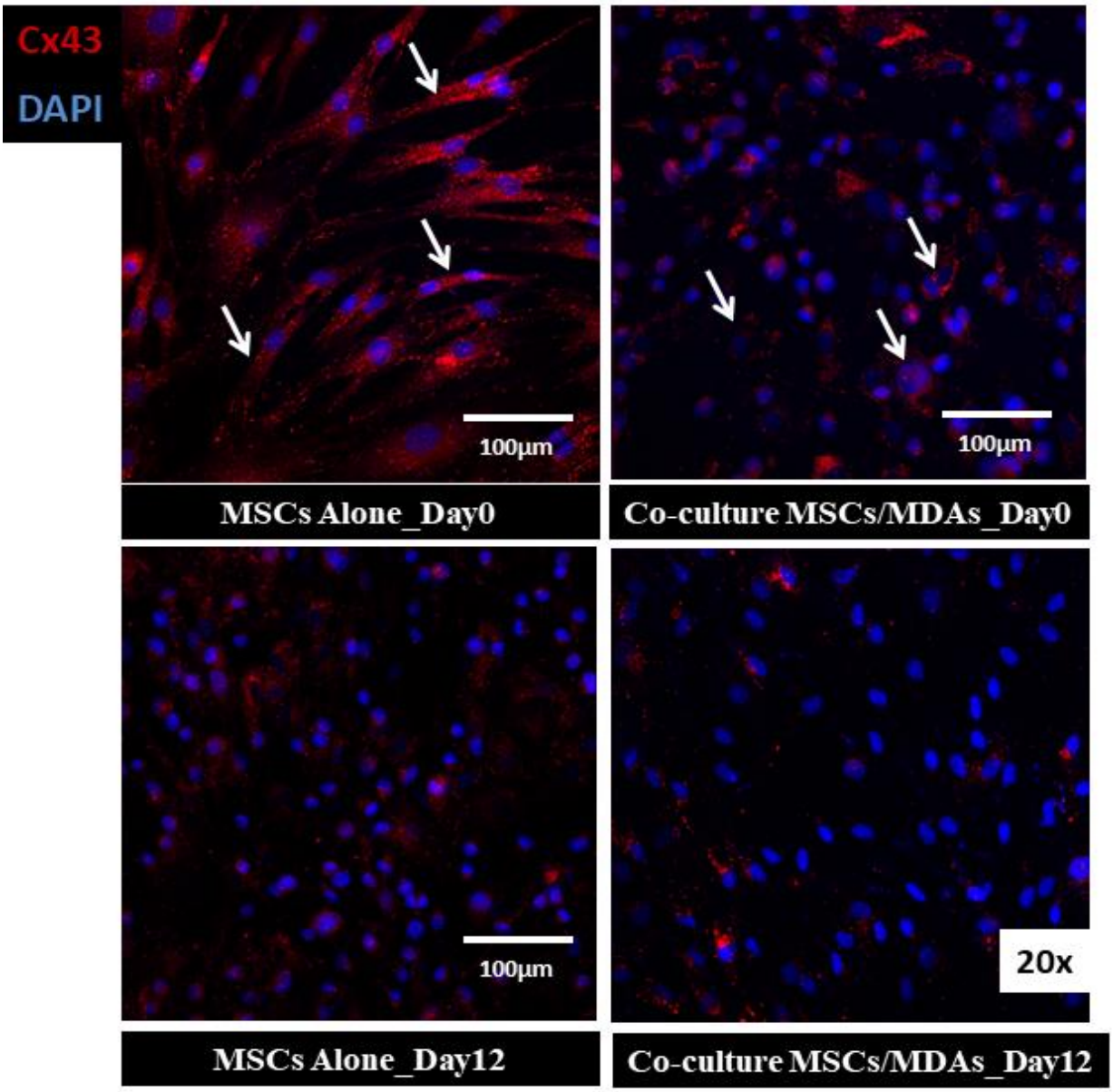

Figure 19. Immunofluorescence images of mesenchymal stem cells co-cultered with MDAs (20x). Images showed a decrease in the expression of cx43 in MSCs post-co-culture with MDAs at both day0 and day12. Cx43 decrease is much more significant at day12. White arrows indicate the morphological changes of MSCs up on co-culture with MDAs . MSCs alone showed a spindle shaped structure, which switches into irregular structure after co-culture.

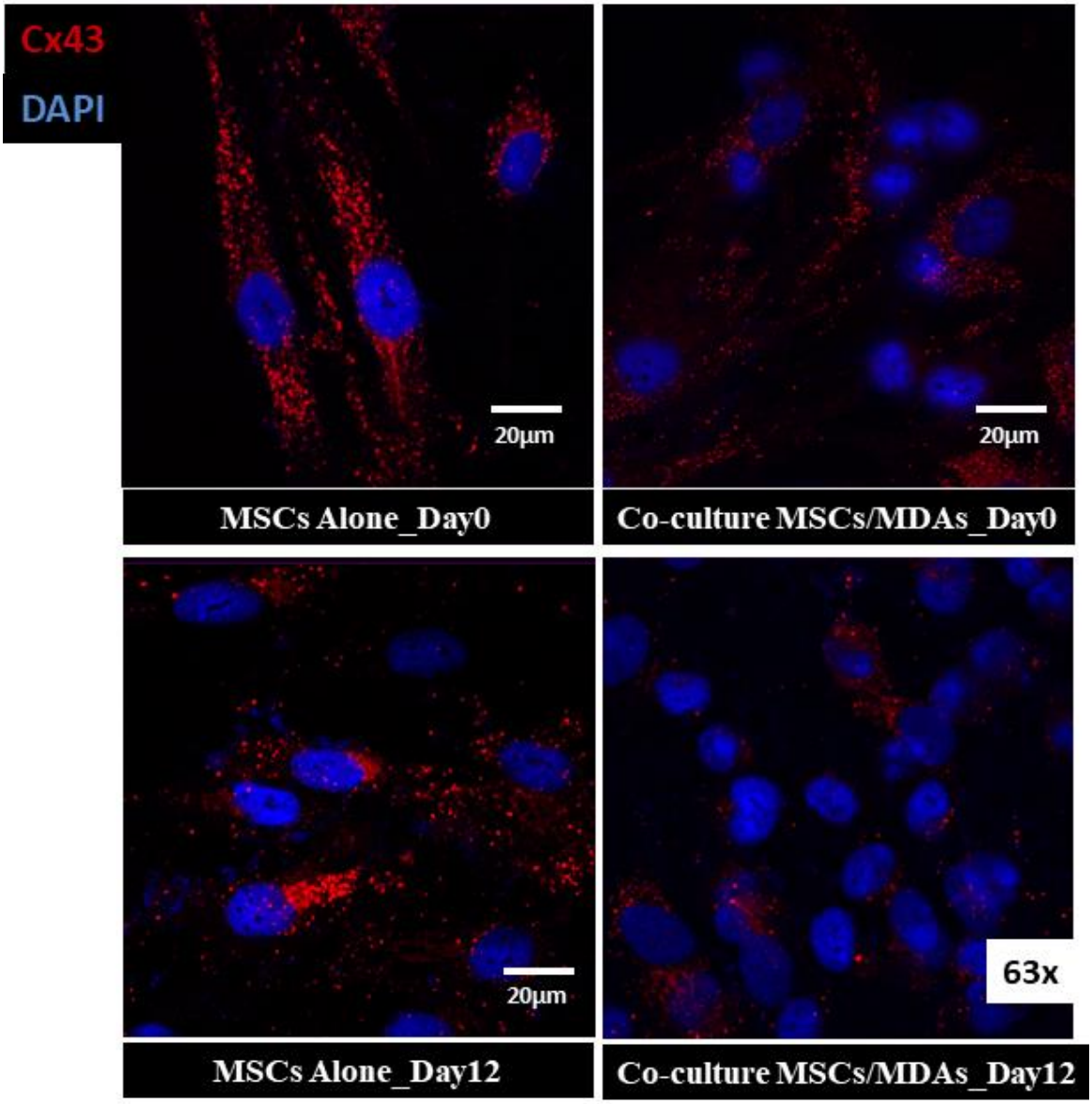

Figure 20. Immunofluorescence images of mesenchymal stem cells co-cultered with MDAs (63x,Oil). Images showed a decrease in the expression of cx43 in MSCs post-co-culture with PC3s at both day0 and day12. Cx43 decrease is much more significant at day12.

I. Assessemnet of N-Cad Expression

Cadherin family is a main interplay in holding cell-cell adehion. Hence, might be playing a key role in maintaining MSCs to cancer cells adhesion.

1. Decrease of N-Cad Expression in MSCs co-cultured with PC3s

In order to evaluate molecular vaiations in MSCs co-cultured with PC3s, N-Cad expression at the genetic and protein level, we performed qRT-PCR, Western Blot analysis and immunofluorescnce assyas on sorted MSCs before and after co-culture at day0 and day12.

N-Cad expression in sorted MSCS decreases up on co-culture at day0 by approximately 3 folds as shown in Figure21-A-1. Similarly,N-Cad expression in sorted MSCs decreases up on co-culture at day12 by approximately 5 folds as shown in Figure21-A-2.

The decrease on day12 with $P_{value} = 0.0006$ is more significant than day0 with $P_{value} = 0.1755$.

This was also confirmed by western blot analysis, as shown in Figure21-B, cx43 protein expression decreases at both day0 and 12 up on co-culture, but more significantly at day12.

Immunofluorescence images reflect a decrease in N-Cad expression in MSCs up on co-culture with PC3s at day0 and day12. Decrease in cx43 expression is more significant up on co-culture at day12 compared to day0, as shown in Figures 22 and 23.

At the morphological level, we can clearly distinguish a switch in the spindle shape of MSCs toward round-shaped morphology post co-culture.

In addition, at day 12 we detected a clear loss of spindle shape MSCs, this is due to DAG assay, ensuring a partial differentiation of MSCs into osteoblasts-like cells during 12 days (as indicated by arrows). .

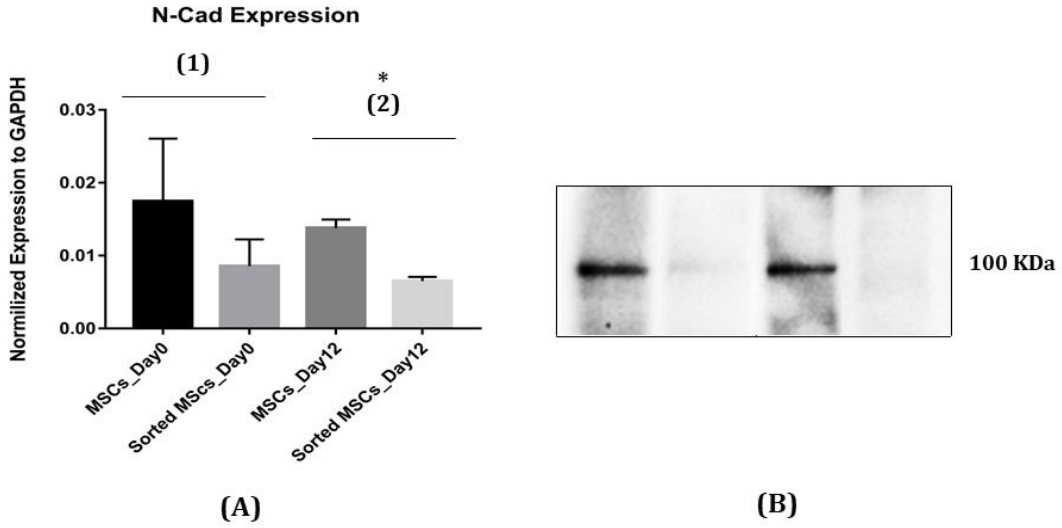

Figure 21. Gene and protein expression of N-Cad in sorted mesenchymal stem cells co-cultered with PC3s. A): Graphical representation of changes in mRNA expression level normalized to GAPDH housekeeping gene showed a decrease in the expression of N-Cad in MSCs up on co-culture with PC3s in both time points: day 0 and 12. (A1): 61% decrease in N-Cad expression up on co-culture of MSCs with PC3s at day0, (A2): 74% decrease in N-Cad expression up on co-culture of MSCs with PC3s at day12. (B): Western blot analysis showed similarly a much more considerable decrease in N-Cad expression on day12 than day0

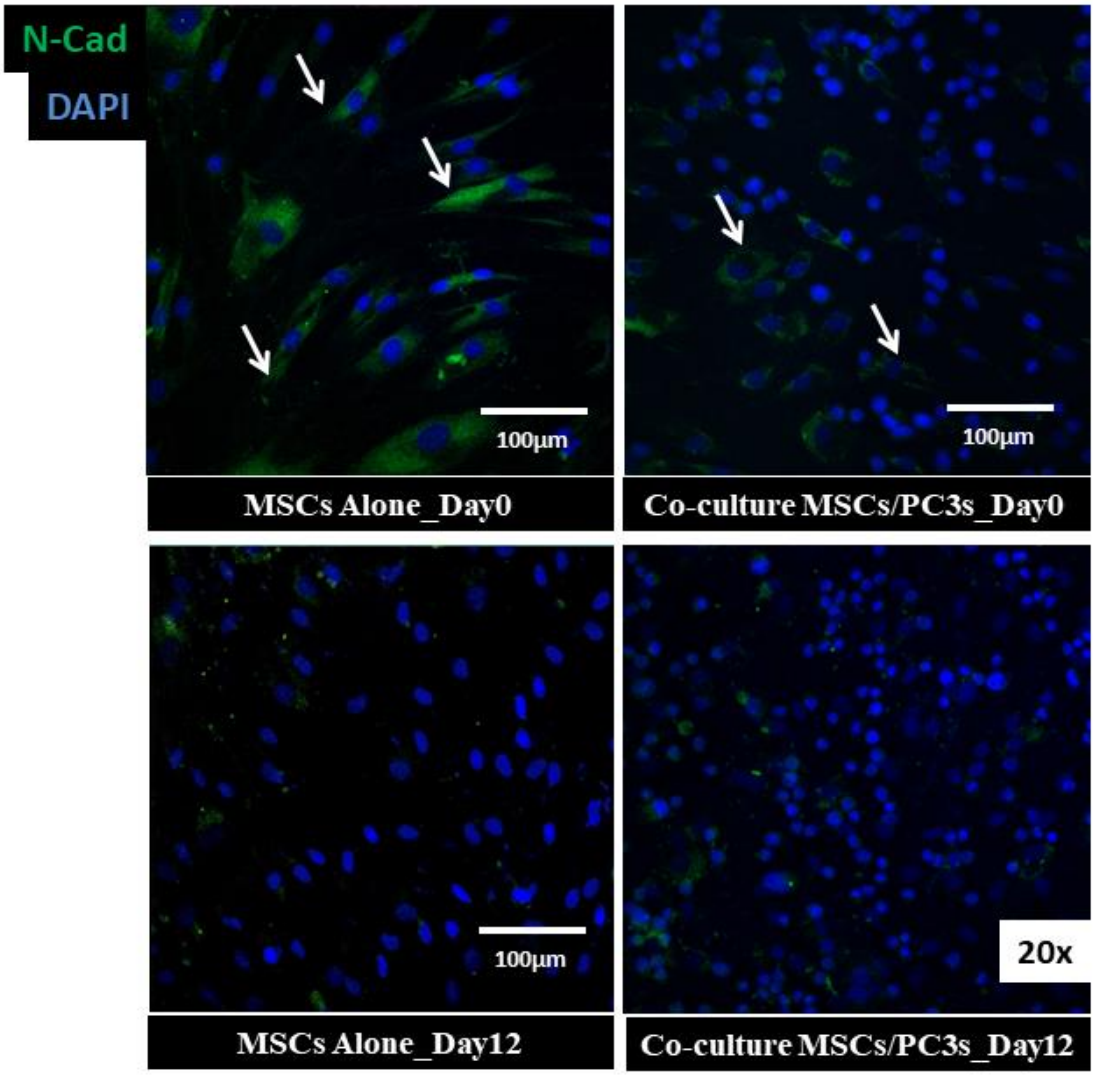

Figure 22. Immunofluorescence images of mesenchymal stem cells co-cultered with PC3s (20x). Images showed a decrease in the expression of N-Cad in MSCs post-co-culture with PC3s at both day0 and day12. N-Cad decrease is much more significant at day12. White arrow indicate the morphological changes of MSCs up on co-culture with PC3s . MSCs alone showed a spindle shaped structure, which switches into irregular structure after co-culture.

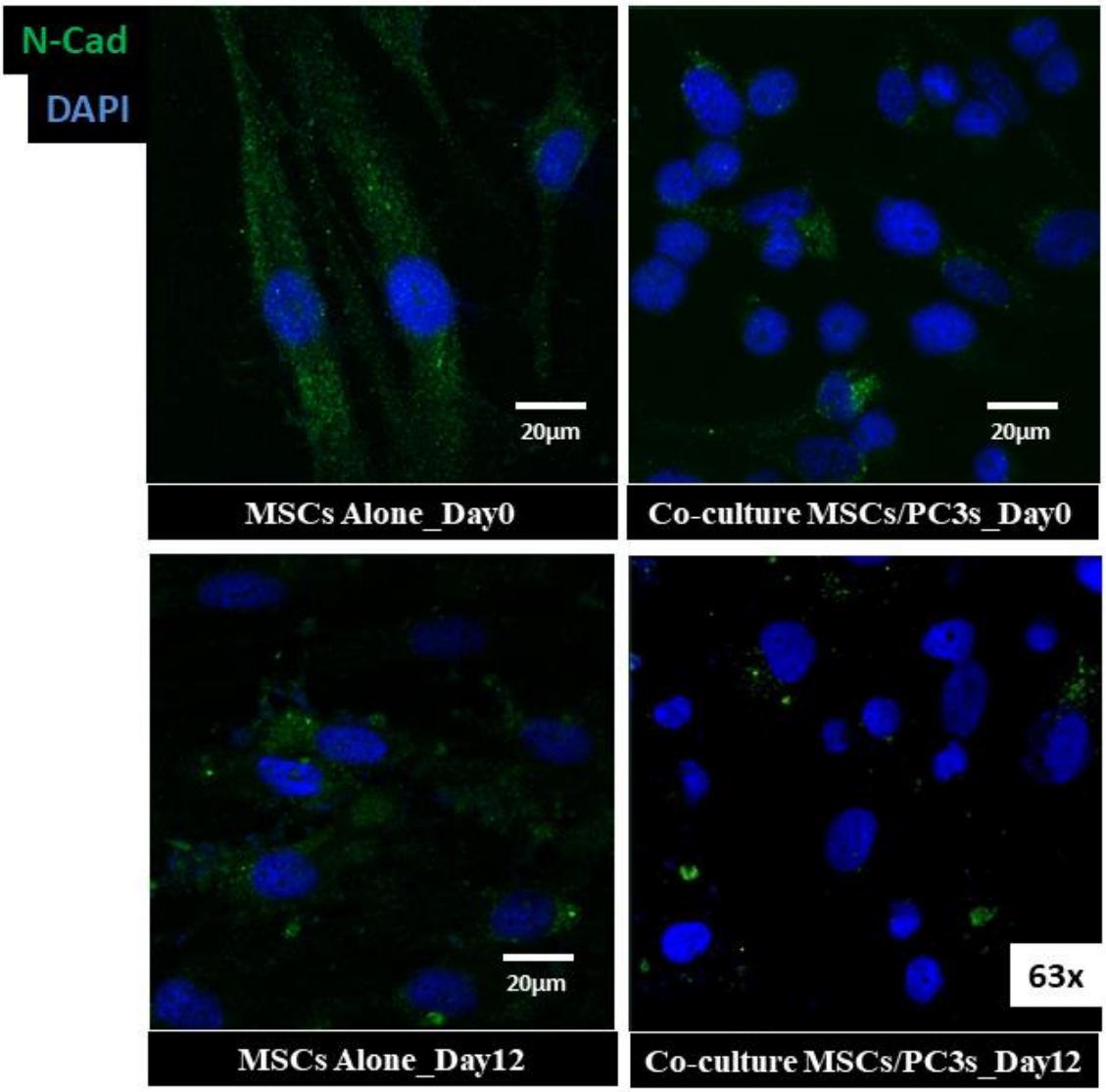

Figure 23. Immunofluorescence images of mesenchymal stem cells co-cultered with PC3s (63x,Oil). Images showed a decrease in the expression of N-Cad in MSCs post-co-culture with PC3s at both day0 and day12. N-Cad decrease is much more significant at day12.

2. Decrease of N-Cad Expression in MSCs co-cultured with MDAs

In order to evaluate molecular vaiations in MSCs co-cultured with MDAs, N-Cad expression at the genetic and protein level, we performed qRT-PCR, Western Blot analysis and immunofluorescnce assyas on sorted MSCs before and after co-culture at day0 and day12.

N-Cad expression in sorted MSCS decreases up on co-culture at day0 by approximately 2 folds as shown in Figure24-A-1. Similarly, N-Cad expression in sorted MSCs decreases up on co-culture at day12 by approximately 10 folds, as shown in Figure24-A-2.

The decrease on day12 with $P_{value} = 0.0003$ is more significant than day0 $P_{value} = 0.0159$.

Immunofluorescence images reflect a decrease in N-Cad expression in MSCs up on co-culture with MDAs at day0 and day12. Decrease in N-Cad expression is more significant up on co-culture at day12 compared to day0, as shown in Figures 25 and 26. At the morphological level, we can clearly distinguish a switch in the spindle shape of MSCs toward round-shaped morphology post co-culture.

In addition, at day 12 we detected a clear loss of spindle shape MSCs, this is due to DAG assay, ensuring a partial differentiation of MSCs into osteoblasts-like cells during 12 days (as indicated by arrows).

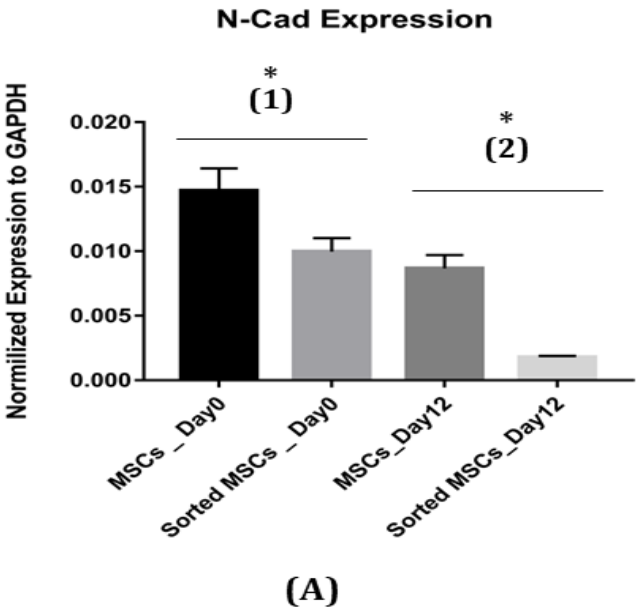

Figure 24. Graphical representation of changes in N-Cad mRNA expression level normalized to GAPDH. Housekeeping gene showed a decrease in the expression of N-Cad in MSCs up on co-culture with PC3s in both time points: day 0 and 12. (A1): 31.27% decrease in N-Cad expression up on co-culture of MSCs with MDAs at day0, (A2): 79% decrease in N-Cad expression up on co-culture of MSCs with MDAs at day12.

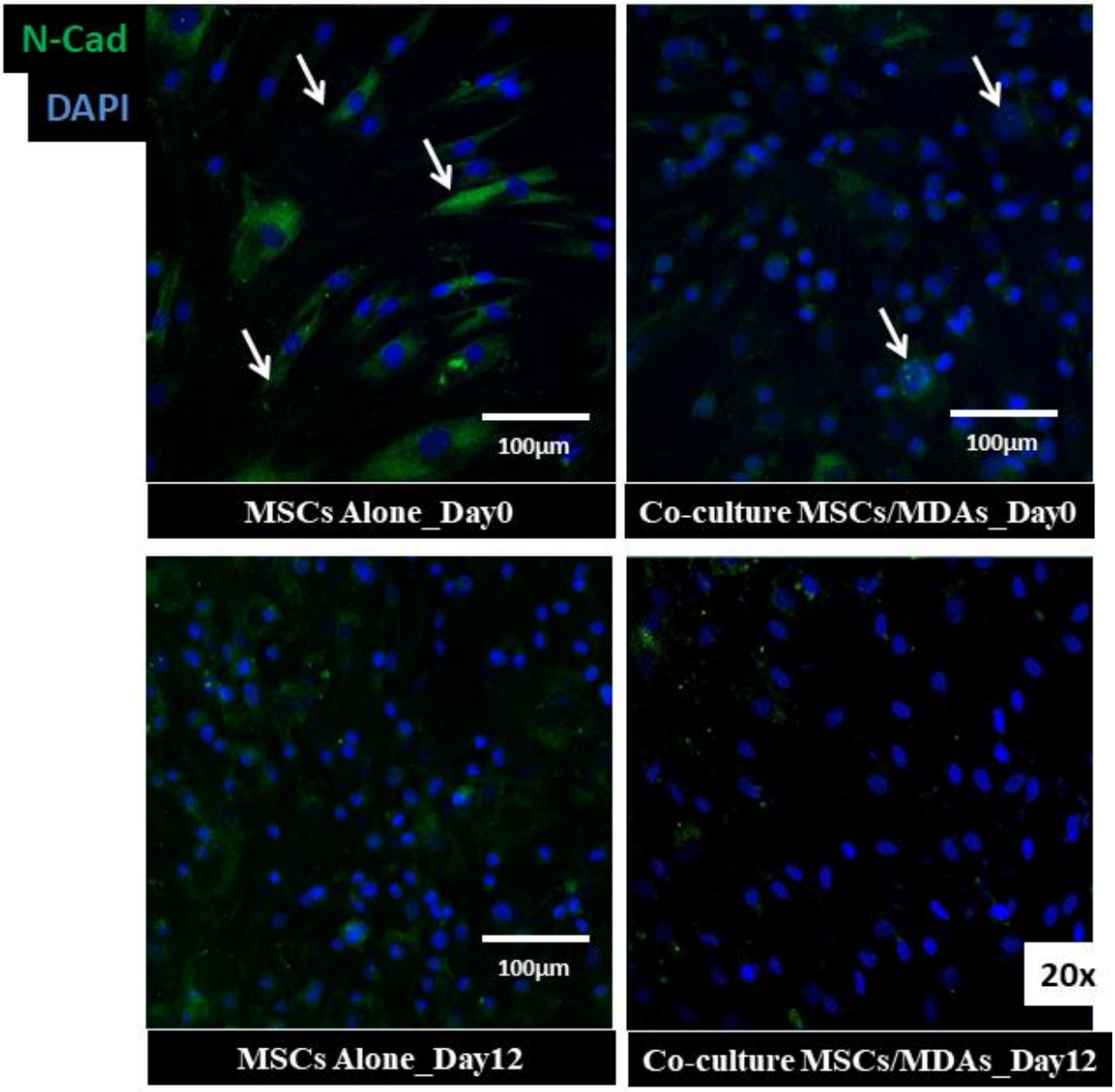

Figure 25. Immunofluorescence images of mesenchymal stem cells co-cultered with MDAs (20x). Images showed a decrease in the expression of N-Cad in MSCs post-co-culture with MDAs at both day0 and day12. N-Cad decrease is much more significant at day12. White arrow indicate the morphological changes of MSCs up on co-culture with MDAs . MSCs alone showed a spindle shaped structure, which switches into irregular structure after co-culture.

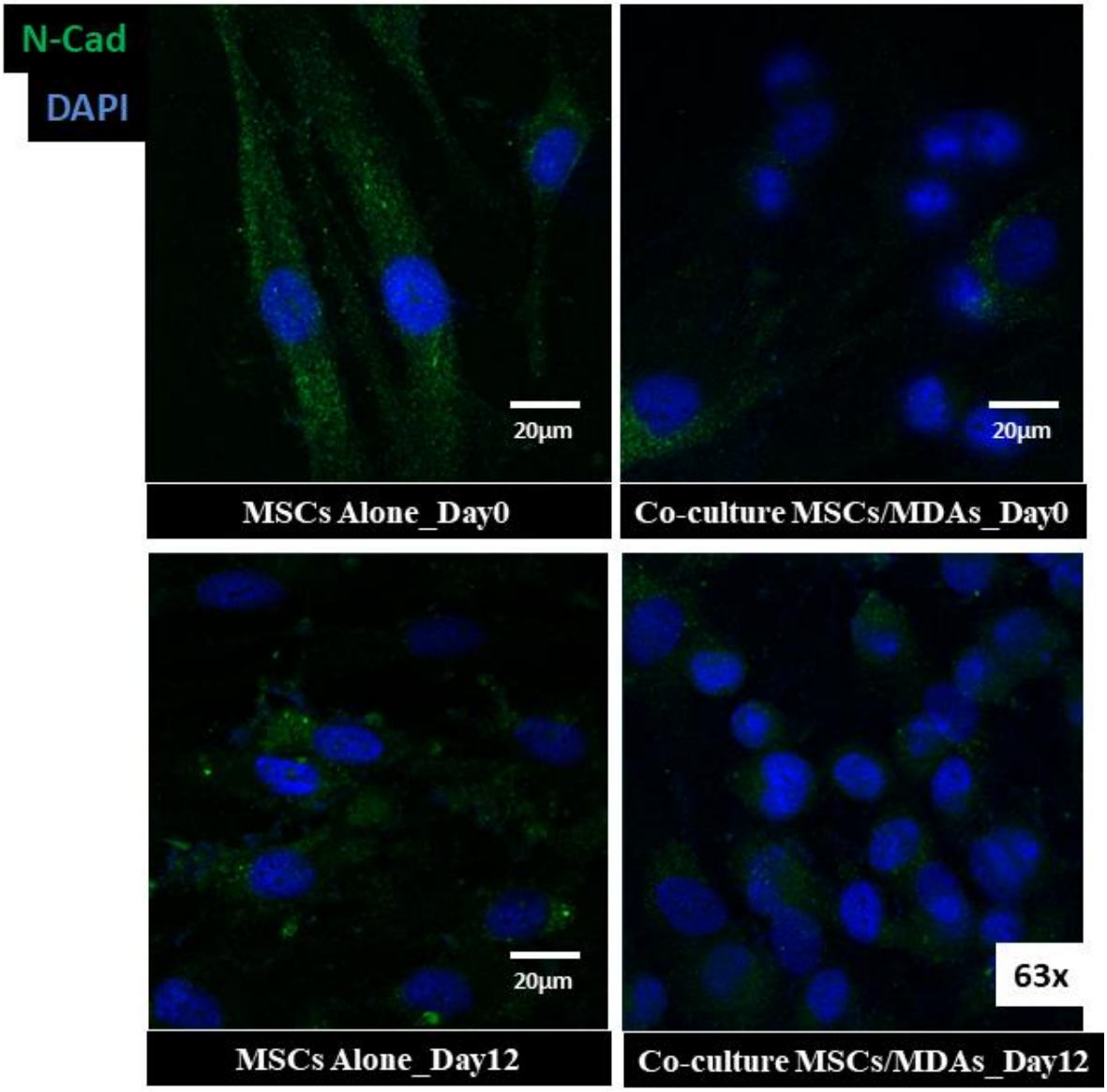

Figure 26. Immunofluorescence images of mesenchymal stem cells co-cultered with MDAs (63x,Oil). Images showed a decrease in the expression of N-Cad in MSCs post-co-culture with MDAs at both day0 and day12. N-Cad decrease is much more significant at day12.

J. E-Cad Expression in sorted MSCs post-co-culture with PC3s and MDAs

Along with cancer progression, MSCs lose their metastatic potential and switch into epithelial cells. In order to assess if the decrease in N-Cad expression is due to MSCs transition into epithelial cells, we performed qRT-PCR targetting E-Cad expression on sorted MSCs before and after co-culture at day0 and day12.

In both sorted MSCs co-cultured with PC3s and MDAs, E-Cad expression increaes on day 12.

As shown in Figure27-A1, E-Cad expression in sorted MSCS increases up on co-culture at day0 by approximately 1.5 folds. Similarly, as shown in Figure27-A2, N-Cad expression in sorted MSCs decreases up on co-culture at day12 by approximately 7 folds.

MSCs co-cultured with PC3s had a very significant increase of E-Cad expression on day 12 with $P_{Value=}\ 0.0001$ compared to day0 with $P_{Value=}\ 0.2125$.

MSCs co-cultured with MDAs had a significant increase of E-Cad expression on day 12 with $P_{Value=}\ 0.0162$ compared to day0 with $P_{Value=}\ 0.0358$.

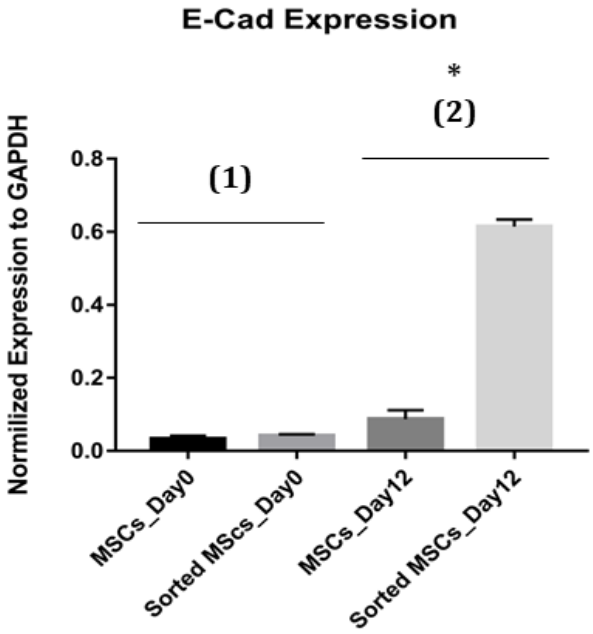

Figure 27. Graphical representation of changes in E-Cad mRNA expression level normalized to GAPDH Housekeeping gene showed a decrease in the expression of E-Cad in MSCs up on co-culture with PC3s in both time points: day 0 and 12. (A1): 19.91% decrease in N-Cad expression up on co-culture of MSCs with PC3s at day0, (A2): 85.85% increase in N-Cad expression up on co-culture of MSCs with PC3s at day12.

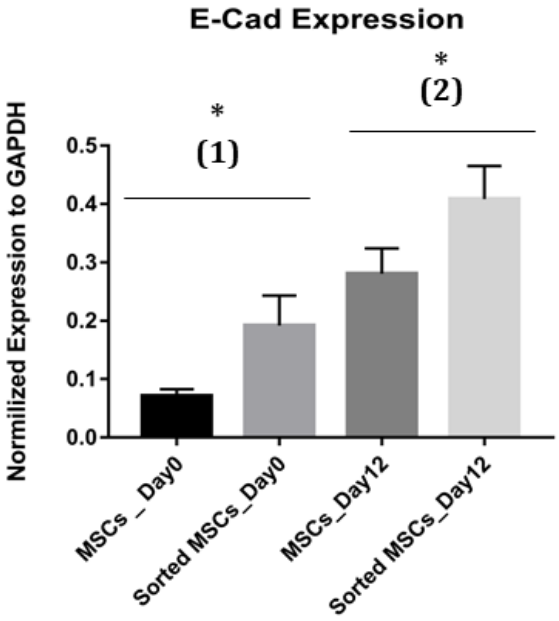

Figure 28. Graphical representation of changes in E-Cad mRNA expression level normalized to GAPDH Housekeeping gene showed a decrease in the expression of N-Cad in MSCs up on co-culture with MDAs in both time points: day 0 and 12. (A1): 41% decrease in E-Cad expression up on co-culture of MSCs with MDAs at day0, (A2): 65.33% decrease in E-Cad expression up on co-culture of MSCs with MDAs at day12.

CHAPTER V

DISCUSSION

Compared to benign tumors, malignant tumors are cancerous. They are often resistant to treatment and may spread to other parts of the body. This is known as metastasis. It is the primary cause of cancer morbidity and mortality. Metastasis involves a series of sequential and interrelated steps. Currently, several hypotheses have been advanced to explain the origin of cancer metastasis. These involve an epithelial mesenchymal transition, an accumulation of mutations in stem cells, a macrophage facilitation process.Every step in the metastatic cascade is cell-cell interactions-dependent [86]. Studies showed that tumor cells express adhesion molecules to maintain their metastatic dissemination[87]. It starts in the primary tumor site where cancer cells proliferate. They increase in number such as in mass. Tumor-induced hypoxia drives the stimulation of microenvironment vascularization by the secretion of pro-angiogenic mediators mainly VEGF, TGF-β, TNF-α, FGF (Fibroblast Growth Factor) and IL-8. So the microenvironment is now invaded. Along with this progression, epithelial cells lose their polarity in addition to their adhesion capacities, modify their apical-basal polarity, re-arrange their cytoskeletal system transforming into mesenchymal multipotent cells capable of differentiating into several cell types. This mechanism is known as EMT activating the transcription of associated genes such as Twist, ZEB, Slug and Snail. So being able to move now,cancer cells detach from the primary microenvironment, itravasating into the circulation. And this is a very key limiting step because less than

0.01% of CTCs succeed seeding the secondary tumor site escaping immune defense, shear stress of blood flow, oxidative stress and end up residing in a new vital niche. CTCs dissemination in a specific secondary tumor site is soil-dependent. They extravasate and again colonize the microenvironment. Bone is the third most common metastatic site for several solid tumors [83]. Prostate and breast cancer cells demonstrate differential propensity in colonizing bone tissue [84, 108]. Metastatic prostate and breast cancer cells have both a marked predilection to colonize bone marrow niche. Cancer metastasis develops in 70% of prostate cancer patients and account for the majority of cancer-related deaths. For breast cancer patients, the case is less aggressive where 12% of patients develop cancer metastasis. Both breast and prostate cancer cells metastasize to the bone following the parallel progression model during their bone microenvironment invasion. Prostate cancer cells show higher tendency homing to the bone[108]. Metastatic tumor cells adhere, interact and cross the endothelial barrier reaching bone internal microenvironment [151]. Maintained by intercellular, intracellular and extracellular signals within the bone niche, metastatic cells interact with bone cells including several cell types at different differentiation states [10]. MSCs residing in the bone microenvironment, with high self-renewal potential are progenitor multipotent cells capable of differentiating into mature osteoblasts [93].

Assuming that bone is constantly formed of specific set of cells uniformly distributed all over the body, CT-Scans of prostate cancer patients in advanced stages revealed region-specific metastatic nodules rather than non-specific nodules distributed all over the body as well [166].

In this study we have aimed to understand the cellular and molecular mechanism that govern prostate and breast cancer cells homing to the bone. We suggested that metastatic cancer cells adhere to a specific class of cells within bone tissues, so that we evaluated the adhesion of MSCs and MSCs induced to differentiate into osteoblastic lineage to both cancer cells, prostate and breast cancer cells.

We established an in vitro model of co-cultured MSCs and MSCs induced to differentiate into osteoblastic lineage. MSCs and partially differentiated MSCs were co-cultured with cancer cells for 30 minutes in a ratio of ½. We trapped the system at different time points. Day12 displayed a maximum adhesion state.

The highest adhesion affinity at day12 was verified by sorting, where the percentage of adherent PC3s increased from 18% at day0 to 36.20% at day12. Linear results, but less significant were detected with MDAs, where the adhesion percentage increased also but slightly from 14.2% at day0 to 16.4% at day12. This ascertains a differential metastatic potential between PC3s and MDAs homing to the bone.

Differentiated MSCs are more appealing for metastatic cancer cells. Indeed, cancer cells revealed highest tendency in adhering to differentiated rather undifferentiated MSCs. Cell-Cell interactions are maintained by an array of intercellular structures such as gap junctions, adherens junctions and tight junctions. Gap junctions maintain intercellular communications and preserve cell-cell exchange, although, count for a minor portion of adhesiveness[140]. However, both tight junctions and adherens junctions contribute for the major adhesiveness fraction. Indeed, one of the most dynamic and effective adhesion mediators is cadherin (cadherin-1 or CDH1) [26, 141]

Among cell-cell adhesion molecules, intercellular communication by gap junctions is paramount for maintaining cellular homeostasis and function. To further explore the molecular and cellular mechanisms maintaining MSCs to cancer cells adhesion, we evaluated the expression of fundamental adhesion markers such as cx43 and N-Cad in MSCs before and after co-culture at day0 and 12. Studies have demonstrated that the inhibition of cadherin function interrupts the formation of gap junctions[148] . Reciprocally, the inhibition of connexin43 disrupts adherens junction formation[157]. Cadherins are transmembrane glycoproteins. They regulate cell adhesion and motility[140]. CTCs dissemination in bone microenvironment is monitored by interactions between E-cadherin (CDH1) of tumor cells - N-cadherin (CDH2).

Gene expression assay, Immunoblotting and immunofluorescence assays showed a decrease in Cx43 and N-Cad expression in MSCs after co-culture with cancer cells at both day0 and day12. The drop in cx43 and N-Cad expression is much more significant in sorted MSCs after co-culture at day12 and in MSCs co-cultured with PC3s more than those co-cultured with MDAs.

Loss of cx43 expression as well as N-Cad is a manifestation of gap junctions and cadherens junctions' loss. Hence, we evaluated E-Cad expression in MSCs at day0 and 12 before and after co-culture with PC3s and MDAs. qRT-PCR showed an up regulation of and E-Cad in sorted MSCs up on co-culture with cancer cells. This increase in E-Cad expression is much more significant in sorted MSCs at day12 and in MSCs co-cultured with PC3s more than those co-cultured with MDAs.

MSCs induced differentiation into osteoblastic lineage: cancer cells adhesion maintenance seems to be cx43, N-Cad independent. Further needs to be done in order to explore more adhesion molecules responsible for adhesion preservation.

All in all, in conclusion, MSCs induced to differentiate into osteoblastic lineage showed higher propensity to sustain cancer cells adhesion. In addition, MSCs induced to differentiate into osteoblastic lineage co-cultured with cancer cells displayed remarkable shift in molecular expression of cx43, N-Cad and E-Cad than undifferentiated MSCs. MSCs induced to differentiate into osteoblastic lineage up on being co-cultured with cancer cells, lose their cx43 and N-Cad expression and increases their epithelial marker E-Cad.

BIBLIOGRAPHY

1. <The age of cancer..pdf>.
2. Spano, D., et al., Molecular networks that regulate cancer metastasis. Semin Cancer Biol, 2012. **22**(3): p. 234-49.
3. Kim, M.Y., et al., Tumor self-seeding by circulating cancer cells. Cell, 2009. **139**(7): p. 1315-26.
4. Langley, R.R. and I.J. Fidler, The seed and soil hypothesis revisited--the role of tumor-stroma interactions in metastasis to different organs. Int J Cancer, 2011. **128**(11): p. 2527-35.
5. Reichert, J.C., et al., Mineralized human primary osteoblast matrices as a model system to analyse interactions of prostate cancer cells with the bone microenvironment. Biomaterials, 2010. **31**(31): p. 7928-36.
6. <1989_Article_StephenPagetSPaperReproducedFr.pdf>.
7. <Neoplastic Diseases.pdf>.
8. Freeman, A.K., V.P. Sumathi, and L. Jeys, Metastatic tumours of bone. Surgery (Oxford), 2018. **36**(1): p. 35-40.
9. Calbo, J., et al., A functional role for tumor cell heterogeneity in a mouse model of small cell lung cancer. Cancer Cell, 2011. **19**(2): p. 244-56.
10. Peinado, H., et al., Pre-metastatic niches: organ-specific homes for metastases. Nat Rev Cancer, 2017. **17**(5): p. 302-317.
11. Aceto, N., et al., Circulating tumor cell clusters are oligoclonal precursors of breast cancer metastasis. Cell, 2014. **158**(5): p. 1110-1122.
12. <Direct signaling between platelets and cancer cells induces an epithelial-mesenchymal-like transition and promotes metastasis 32.pdf>.
13. Husemann, Y., et al., Systemic spread is an early step in breast cancer. Cancer Cell, 2008. **13**(1): p. 58-68.
14. Weinberg, R.A., Leaving home early: reexamination of the canonical models of tumor progression. Cancer Cell, 2008. **14**(4): p. 283-4.
15. Sanger, N., et al., Disseminated tumor cells in the bone marrow of patients with ductal carcinoma in situ. Int J Cancer, 2011. **129**(10): p. 2522-6.
16. Janssen, L.M.E., et al., The immune system in cancer metastasis: friend or foe? J Immunother Cancer, 2017. **5**(1): p. 79.
17. Lu, X. and Y. Kang, Chemokine (C-C motif) ligand 2 engages CCR2+ stromal cells of monocytic origin to promote breast cancer metastasis to lung and bone. J Biol Chem, 2009. **284**(42): p. 29087-96.
18. Li, X., et al., A Destructive Cascade Mediated by CCL2 Facilitates Prostate Cancer Growth in Bone. Cancer Research, 2009. **69**(4): p. 1685-1692.
19. Luo, X., et al., Stromal-Initiated Changes in the Bone Promote Metastatic Niche Development. Cell Rep, 2016. **14**(1): p. 82-92.
20. Sethi, N., et al., Tumor-derived JAGGED1 promotes osteolytic bone metastasis of breast cancer by engaging notch signaling in bone cells. Cancer Cell, 2011. **19**(2): p. 192-205.

21. Costa-Silva, B., et al., Pancreatic cancer exosomes initiate pre-metastatic niche formation in the liver. Nat Cell Biol, 2015. **17**(6): p. 816-26.
22. Hanahan, D. and R.A. Weinberg, Hallmarks of cancer: the next generation. Cell, 2011. **144**(5): p. 646-74.
23. Kusumbe, A.P., Vascular niches for disseminated tumour cells in bone. J Bone Oncol, 2016. **5**(3): p. 112-116.
24. Rajabi, M. and S.A. Mousa, The Role of Angiogenesis in Cancer Treatment. Biomedicines, 2017. **5**(2).
25. Winkler, F., Hostile takeover: how tumours hijack pre-existing vascular environments to thrive. J Pathol, 2017. **242**(3): p. 267-272.
26. Bogenrieder, T. and M. Herlyn, Axis of evil: molecular mechanisms of cancer metastasis. Oncogene, 2003. **22**(42): p. 6524-36.
27. Kamba, T. and D.M. McDonald, Mechanisms of adverse effects of anti-VEGF therapy for cancer. Br J Cancer, 2007. **96**(12): p. 1788-95.
28. Boucher, J., et al., Connexins, important players in the dissemination of prostate cancer cells. Biochim Biophys Acta Biomembr, 2018. **1860**(1): p. 202-215.
29. Thiery, J.P., et al., Epithelial-mesenchymal transitions in development and disease. Cell, 2009. **139**(5): p. 871-90.
30. Kalluri, R., EMT: when epithelial cells decide to become mesenchymal-like cells. J Clin Invest, 2009. **119**(6): p. 1417-9.
31. Kang, Y. and J. Massague, Epithelial-mesenchymal transitions: twist in development and metastasis. Cell, 2004. **118**(3): p. 277-9.
32. Polyak, K. and R.A. Weinberg, Transitions between epithelial and mesenchymal states: acquisition of malignant and stem cell traits. Nat Rev Cancer, 2009. **9**(4): p. 265-73.
33. Stockinger, A., et al., E-cadherin regulates cell growth by modulating proliferation-dependent beta-catenin transcriptional activity. J Cell Biol, 2001. **154**(6): p. 1185-96.
34. Trimboli, A.J., et al., Direct evidence for epithelial-mesenchymal transitions in breast cancer. Cancer Res, 2008. **68**(3): p. 937-45.
35. Thiery, J.P. and J.P. Sleeman, Complex networks orchestrate epithelial-mesenchymal transitions. Nat Rev Mol Cell Biol, 2006. **7**(2): p. 131-42.
36. Zhou, C., et al., Inflammation linking EMT and cancer stem cells. Oral Oncol, 2012. **48**(11): p. 1068-75.
37. Scheel, C., et al., Paracrine and autocrine signals induce and maintain mesenchymal and stem cell states in the breast. Cell, 2011. **145**(6): p. 926-40.
38. <Hedgehog signalling in prostate regeneration, neoplasia and metastasis.pdf>.
39. <Migrating cancer stem cells — an integrated concept of malignant tumour progression.pdf>.
40. Zhu, S., J.D. Bjorge, and D.J. Fujita, PTP1B contributes to the oncogenic properties of colon cancer cells through Src activation. Cancer Res, 2007. **67**(21): p. 10129-37.
41. Dolcetti, L., et al., Hierarchy of immunosuppressive strength among myeloid-derived suppressor cell subsets is determined by GM-CSF. Eur J Immunol, 2010. **40**(1): p. 22-35.

42. Prasad, S., et al., Inflammatory processes have differential effects on claudins 2, 3 and 4 in colonic epithelial cells. Lab Invest, 2005. **85**(9): p. 1139-62.
43. Koh, B.I. and Y. Kang, The pro-metastatic role of bone marrow-derived cells: a focus on MSCs and regulatory T cells. EMBO Rep, 2012. **13**(5): p. 412-22.
44. Tlsty, T.D. and L.M. Coussens, Tumor stroma and regulation of cancer development. Annu Rev Pathol, 2006. **1**: p. 119-50.
45. <Epithelial-Mesenchymal Transition in tumor microenvironment .pdf>.
46. Fordyce, C.A., et al., Cell-extrinsic consequences of epithelial stress: activation of protumorigenic tissue phenotypes. Breast Cancer Res, 2012. **14**(6): p. R155.
47. Ghajar, C.M., et al., The perivascular niche regulates breast tumour dormancy. Nat Cell Biol, 2013. **15**(7): p. 807-17.
48. Barcellos-Hoff, M.H., D. Lyden, and T.C. Wang, The evolution of the cancer niche during multistage carcinogenesis. Nat Rev Cancer, 2013. **13**(7): p. 511-8.
49. Ruffell, B., et al., Lymphocytes in cancer development: polarization towards pro-tumor immunity. Cytokine Growth Factor Rev, 2010. **21**(1): p. 3-10.
50. Movahedi, K., et al., Identification of discrete tumor-induced myeloid-derived suppressor cell subpopulations with distinct T cell-suppressive activity. Blood, 2008. **111**(8): p. 4233-44.
51. Elkabets, M., et al., IL-1beta regulates a novel myeloid-derived suppressor cell subset that impairs NK cell development and function. Eur J Immunol, 2010. **40**(12): p. 3347-57.
52. Bui, J.D. and R.D. Schreiber, Cancer immunosurveillance, immunoediting and inflammation: independent or interdependent processes? Curr Opin Immunol, 2007. **19**(2): p. 203-8.
53. Garcia-Lora, A., I. Algarra, and F. Garrido, MHC class I antigens, immune surveillance, and tumor immune escape. J Cell Physiol, 2003. **195**(3): p. 346-55.
54. Liao, D., et al., Cancer associated fibroblasts promote tumor growth and metastasis by modulating the tumor immune microenvironment in a 4T1 murine breast cancer model. PLoS One, 2009. **4**(11): p. e7965.
55. Barbosa, C.M., et al., Differentiation of hematopoietic stem cell and myeloid populations by ATP is modulated by cytokines. Cell Death Dis, 2011. **2**: p. e165.
56. Seita, J. and I.L. Weissman, Hematopoietic stem cell: self-renewal versus differentiation. Wiley Interdiscip Rev Syst Biol Med, 2010. **2**(6): p. 640-53.
57. Yan, M. and P. Jurasz, The role of platelets in the tumor microenvironment: From solid tumors to leukemia. Biochim Biophys Acta, 2016. **1863**(3): p. 392-400.
58. Guo, W. and F.G. Giancotti, Integrin signalling during tumour progression. Nat Rev Mol Cell Biol, 2004. **5**(10): p. 816-26.
59. <Antioxidant and oncogene.pdf>.
60. Valastyan, S. and R.A. Weinberg, Tumor metastasis: molecular insights and evolving paradigms. Cell, 2011. **147**(2): p. 275-92.
61. Engl, T., et al., CXCR4 chemokine receptor mediates prostate tumor cell adhesion through alpha5 and beta3 integrins. Neoplasia, 2006. **8**(4): p. 290-301.

62. Kukreja, P., et al., Up-regulation of CXCR4 expression in PC-3 cells by stromal-derived factor-1alpha (CXCL12) increases endothelial adhesion and transendothelial migration: role of MEK/ERK signaling pathway-dependent NF-kappaB activation. Cancer Res, 2005. **65**(21): p. 9891-8.
63. Graham, N. and B.Z. Qian, Mesenchymal Stromal Cells: Emerging Roles in Bone Metastasis. Int J Mol Sci, 2018. **19**(4).
64. Hamidi, H. and J. Ivaska, Every step of the way: integrins in cancer progression and metastasis. Nat Rev Cancer, 2018. **18**(9): p. 533-548.
65. Barthel, S.R., et al., Definition of molecular determinants of prostate cancer cell bone extravasation. Cancer Res, 2013. **73**(2): p. 942-52.
66. Joyce, J.A. and J.W. Pollard, Microenvironmental regulation of metastasis. Nat Rev Cancer, 2009. **9**(4): p. 239-52.
67. Mendez-Ferrer, S., et al., Mesenchymal and haematopoietic stem cells form a unique bone marrow niche. Nature, 2010. **466**(7308): p. 829-34.
68. Zhou, H.S., B.Z. Carter, and M. Andreeff, Bone marrow niche-mediated survival of leukemia stem cells in acute myeloid leukemia: Yin and Yang. Cancer Biol Med, 2016. **13**(2): p. 248-59.
69. Oskarsson, T., Extracellular matrix components in breast cancer progression and metastasis. Breast, 2013. **22 Suppl 2**: p. S66-72.
70. Cordeiro-Spinetti, E., R.S. Taichman, and A. Balduino, The bone marrow endosteal niche: how far from the surface? J Cell Biochem, 2015. **116**(1): p. 6-11.
71. Weilbaecher, K.N., T.A. Guise, and L.K. McCauley, Cancer to bone: a fatal attraction. Nat Rev Cancer, 2011. **11**(6): p. 411-25.
72. Zhang, X.H., et al., Latent bone metastasis in breast cancer tied to Src-dependent survival signals. Cancer Cell, 2009. **16**(1): p. 67-78.
73. Kolb, A.D. and K.M. Bussard, The Bone Extracellular Matrix as an Ideal Milieu for Cancer Cell Metastases. Cancers (Basel), 2019. **11**(7).
74. <41.pdf>.
75. <Tumor Necrosis Factora 39.pdf>.
76. Yang, C.M., et al., Mechanical strain induces collagenase-3 (MMP-13) expression in MC3T3-E1 osteoblastic cells. J Biol Chem, 2004. **279**(21): p. 22158-65.
77. Teti, A., Bone development: overview of bone cells and signaling. Curr Osteoporos Rep, 2011. **9**(4): p. 264-73.
78. <Osteoprotegerin Ligand Is a Cytokine that Regulates Osteoclast Differentiation and Activation.pdf>.
79. Bruzzaniti, A. and R. Baron, Molecular regulation of osteoclast activity. Rev Endocr Metab Disord, 2006. **7**(1-2): p. 123-39.
80. <Development of the osteoblast phenotype molecular mechanisms mediating osteoblast.pdf>.
81. Xiao, W., et al., Cellular and Molecular Aspects of Bone Remodeling. Front Oral Biol, 2016. **18**: p. 9-16.
82. Wu, M.Y., et al., Molecular Regulation of Bone Metastasis Pathogenesis. Cell Physiol Biochem, 2018. **46**(4): p. 1423-1438.

83. Hernandez, R.K., et al., Incidence of bone metastases in patients with solid tumors: analysis of oncology electronic medical records in the United States. BMC Cancer, 2018. **18**(1): p. 44.
84. Hensel, J. and G.N. Thalmann, Biology of Bone Metastases in Prostate Cancer. Urology, 2016. **92**: p. 6-13.
85. Johnson, R.W., M.E. Sowder, and A.J. Giaccia, Hypoxia and Bone Metastatic Disease. Curr Osteoporos Rep, 2017. **15**(4): p. 231-238.
86. Arai, F., et al., Tie2/angiopoietin-1 signaling regulates hematopoietic stem cell quiescence in the bone marrow niche. Cell, 2004. **118**(2): p. 149-61.
87. Schneider, J.G., S.R. Amend, and K.N. Weilbaecher, Integrins and bone metastasis: integrating tumor cell and stromal cell interactions. Bone, 2011. **48**(1): p. 54-65.
88. Kang, Y., et al., A multigenic program mediating breast cancer metastasis to bone. Cancer Cell, 2003. **3**(6): p. 537-549.
89. You, J.S. and P.A. Jones, Cancer genetics and epigenetics: two sides of the same coin? Cancer Cell, 2012. **22**(1): p. 9-20.
90. Vanharanta, S., et al., Epigenetic expansion of VHL-HIF signal output drives multiorgan metastasis in renal cancer. Nat Med, 2013. **19**(1): p. 50-6.
91. <Very High Frequency of Hypermethylated Genes in Breast Cancer.pdf>.
92. Vogelstein, B., et al., Cancer genome landscapes. Science, 2013. **339**(6127): p. 1546-58.
93. <Neoplastic Bone Marrow Niche MSC and HSC !!.pdf>.
94. <Multilineage potential of adult human mesenchymal stem cells _ 8.pdf>.
95. Gronthos, S., et al., Postnatal human dental pulp stem cells (DPSCs) in vitro and in vivo. Proc Natl Acad Sci U S A, 2000. **97**(25): p. 13625-30.
96. <Rat Extramedullary Adipose Tissue as a Source of Osteochondrogenic Progenitor Cells _ 13.pdf>.
97. <The development of fibroblast colonies in monolayer cultures of guinea-pig bone marrow and spleen cells _ 14.pdf>.
98. Dominici, M., et al., Minimal criteria for defining multipotent mesenchymal stromal cells. The International Society for Cellular Therapy position statement. Cytotherapy, 2006. **8**(4): p. 315-7.
99. Omatsu, Y., et al., The essential functions of adipo-osteogenic progenitors as the hematopoietic stem and progenitor cell niche. Immunity, 2010. **33**(3): p. 387-99.
100. Kunisaki, Y., et al., Arteriolar niches maintain haematopoietic stem cell quiescence. Nature, 2013. **502**(7473): p. 637-43.
101. Crane, G.M., E. Jeffery, and S.J. Morrison, Adult haematopoietic stem cell niches. Nat Rev Immunol, 2017. **17**(9): p. 573-590.
102. Shiozawa, Y., et al., Human prostate cancer metastases target the hematopoietic stem cell niche to establish footholds in mouse bone marrow. J Clin Invest, 2011. **121**(4): p. 1298-312.
103. Jung, Y., et al., Recruitment of mesenchymal stem cells into prostate tumours promotes metastasis. Nat Commun, 2013. **4**: p. 1795.

104. Lam, H.M., R.L. Vessella, and C. Morrissey, The role of the microenvironment-dormant prostate disseminated tumor cells in the bone marrow. Drug Discov Today Technol, 2014. **11**: p. 41-7.
105. Pietras, K. and A. Ostman, Hallmarks of cancer: interactions with the tumor stroma. Exp Cell Res, 2010. **316**(8): p. 1324-31.
106. Sato, T., et al., Tumor-stromal cell contact promotes invasion of human uterine cervical carcinoma cells by augmenting the expression and activation of stromal matrix metalloproteinases. Gynecol Oncol, 2004. **92**(1): p. 47-56.
107. Chamberlain, G., et al., Concise review: mesenchymal stem cells: their phenotype, differentiation capacity, immunological features, and potential for homing. Stem Cells, 2007. **25**(11): p. 2739-49.
108. <Vascular Endothelial Growth Factor Contributes to the Prostate Cancer-Induced.pdf>.
109. <From latent disseminated cells to overt metastasis genetic analysis of systemic breast cancer progression. 10.pdf>.
110. Weckermann, D., et al., Perioperative activation of disseminated tumor cells in bone marrow of patients with prostate cancer. J Clin Oncol, 2009. **27**(10): p. 1549-56.
111. Pan, H., et al., 20-Year Risks of Breast-Cancer Recurrence after Stopping Endocrine Therapy at 5 Years. N Engl J Med, 2017. **377**(19): p. 1836-1846.
112. Johnson, R.W., E. Schipani, and A.J. Giaccia, HIF targets in bone remodeling and metastatic disease. Pharmacol Ther, 2015. **150**: p. 169-77.
113. Obenauf, A.C. and J. Massague, Surviving at a Distance: Organ-Specific Metastasis. Trends Cancer, 2015. **1**(1): p. 76-91.
114. Minn, A.J., et al., Distinct organ-specific metastatic potential of individual breast cancer cells and primary tumors. Journal of Clinical Investigation, 2005. **115**(1): p. 44-55.
115. David Roodman, G. and R. Silbermann, Mechanisms of osteolytic and osteoblastic skeletal lesions. Bonekey Rep, 2015. **4**: p. 753.
116. Lu, P., et al., Extracellular matrix degradation and remodeling in development and disease. Cold Spring Harb Perspect Biol, 2011. **3**(12).
117. Walker, C., E. Mojares, and A. Del Rio Hernandez, Role of Extracellular Matrix in Development and Cancer Progression. Int J Mol Sci, 2018. **19**(10).
118. Lu, P., V.M. Weaver, and Z. Werb, The extracellular matrix: a dynamic niche in cancer progression. J Cell Biol, 2012. **196**(4): p. 395-406.
119. Buijs, J.T., K.R. Stayrook, and T.A. Guise, The role of TGF-beta in bone metastasis: novel therapeutic perspectives. Bonekey Rep, 2012. **1**: p. 96.
120. Sottnik, J.L., et al., Tumor-induced pressure in the bone microenvironment causes osteocytes to promote the growth of prostate cancer bone metastases. Cancer Res, 2015. **75**(11): p. 2151-8.
121. Kimura, Y., et al., Alteration of osteoblast arrangement via direct attack by cancer cells: New insights into bone metastasis. Sci Rep, 2017. **7**: p. 44824.
122. Sekita, A., A. Matsugaki, and T. Nakano, Disruption of collagen/apatite alignment impairs bone mechanical function in osteoblastic metastasis induced by prostate cancer. Bone, 2017. **97**: p. 83-93.

123. Funa, K., H. Nordgren, and S. Nilsson, In situ expression of mRNA for proto-oncogenes in benign prostatic hyperplasia and in prostatic carcinoma. Scand J Urol Nephrol, 1991. **25**(2): p. 95-100.
124. <The effects of the endothelin family peptides on cultured osteoblastic.pdf>.
125. <Identification of Endothelin.pdf>.
126. <The Role of the Wnt-.pdf>.
127. Guise, T.A., et al., Basic mechanisms responsible for osteolytic and osteoblastic bone metastases. Clin Cancer Res, 2006. **12**(20 Pt 2): p. 6213s-6216s.
128. Bonfil, R.D. and M.L. Cher, The role of proteolytic enzymes in metastatic bone disease. IBMS BoneKEy, 2011. **8**(1): p. 16-36.
129. Phadke, P.A., et al., Kinetics of metastatic breast cancer cell trafficking in bone. Clin Cancer Res, 2006. **12**(5): p. 1431-40.
130. Wang, H., et al., The osteogenic niche promotes early-stage bone colonization of disseminated breast cancer cells. Cancer Cell, 2015. **27**(2): p. 193-210.
131. Ubellacker, J.M., et al., Modulating Bone Marrow Hematopoietic Lineage Potential to Prevent Bone Metastasis in Breast Cancer. Cancer Res, 2018. **78**(18): p. 5300-5314.
132. Lynch, C.C., et al., MMP-7 promotes prostate cancer-induced osteolysis via the solubilization of RANKL. Cancer Cell, 2005. **7**(5): p. 485-96.
133. Lu, X., et al., ADAMTS1 and MMP1 proteolytically engage EGF-like ligands in an osteolytic signaling cascade for bone metastasis. Genes Dev, 2009. **23**(16): p. 1882-94.
134. Bendre, M.S., et al., Interleukin-8 stimulation of osteoclastogenesis and bone resorption is a mechanism for the increased osteolysis of metastatic bone disease. Bone, 2003. **33**(1): p. 28-37.
135. Logothetis, C.J. and S.H. Lin, Osteoblasts in prostate cancer metastasis to bone. Nat Rev Cancer, 2005. **5**(1): p. 21-8.
136. Boucharaba, A., et al., Platelet-derived lysophosphatidic acid supports the progression of osteolytic bone metastases in breast cancer. Journal of Clinical Investigation, 2004. **114**(12): p. 1714-1725.
137. Psaila, B., D. Lyden, and I. Roberts, Megakaryocytes, malignancy and bone marrow vascular niches. J Thromb Haemost, 2012. **10**(2): p. 177-88.
138. Ara, T. and Y.A. Declerck, Interleukin-6 in bone metastasis and cancer progression. Eur J Cancer, 2010. **46**(7): p. 1223-31.
139. <Mechanisms of Bone Metastasis !!!!!.pdf>.
140. <SIGNAL TRANSDUCTION BY CELL ADHESION - 2002.pdf>.
141. Cavallaro, U. and G. Christofori, Cell adhesion and signalling by cadherins and Ig-CAMs in cancer. Nat Rev Cancer, 2004. **4**(2): p. 118-32.
142. Shaw, E., N. Massaro, and N.T. Brockton, The role of vitamin D in hepatic metastases from colorectal cancer. Clin Transl Oncol, 2018. **20**(3): p. 259-273.
143. Mineta, K., et al., Predicted expansion of the claudin multigene family. FEBS Lett, 2011. **585**(4): p. 606-12.
144. <Chronic Exposure of LLC-PK1Epithelia to the Phorbol Ester TPA Produces Polyp-like Foci with Leaky Tight Junctions and Altered Protein Kinase C-α Expression and Localization _ 18.pdf>.

145. Peter, Y., et al., Epidermal growth factor receptor and claudin-2 participate in A549 permeability and remodeling: implications for non-small cell lung cancer tumor colonization. Mol Carcinog, 2009. **48**(6): p. 488-97.
146. <Stimulation of glucose uptake by transforming growth factor beta dence for the requirement of epidermal growth factor-receptor activation. _ 29.pdf>.
147. Kanczuga-Koda, L., et al., Increased expression of connexins 26 and 43 in lymph node metastases of breast cancer. J Clin Pathol, 2006. **59**(4): p. 429-33.
148. <Gap Junction Formation between CulturedEmbryonic Lens Cells Is Inhibitedby Antibody to N-Cadherin.pdf>.
149. Keicher, C., et al., Phosphorylation of mouse LASP-1 on threonine 156 by cAMP- and cGMP-dependent protein kinase. Biochem Biophys Res Commun, 2004. **324**(1): p. 308-16.
150. <Reduced expression of Claudin-7 in fine needle aspirates from breast carcinomas correlate with grading and metastatic disease _ 37.pdf>.
151. <A role for heterologous gap junctions between melanoma and endothelial cells in metastasis - 9 .pdf>.
152. Dhawan, P., et al., Claudin-1 regulates cellular transformation and metastatic behavior in colon cancer. J Clin Invest, 2005. **115**(7): p. 1765-76.
153. Laird, D.W. and P.D. Lampe, Therapeutic strategies targeting connexins. Nat Rev Drug Discov, 2018. **17**(12): p. 905-921.
154. <The Gap Junction Communication Channel - Review -1996.pdf>.
155. Wei, C.J., X. Xu, and C.W. Lo, Connexins and cell signaling in development and disease. Annu Rev Cell Dev Biol, 2004. **20**: p. 811-38.
156. Herve, J.C., N. Bourmeyster, and D. Sarrouilhe, Diversity in protein-protein interactions of connexins: emerging roles. Biochim Biophys Acta, 2004. **1662**(1-2): p. 22-41.
157. <Inhibition of gap junction and adherens _ 1992.pdf>.
158. <Direct Association of the Gap Junction Protein Connexin-43 with 1998.pdf>.
159. Lin, D., et al., Protein kinase Cgamma regulation of gap junction activity through caveolin-1-containing lipid rafts. Invest Ophthalmol Vis Sci, 2003. **44**(12): p. 5259-68.
160. Kazan, J.M., et al., Cx43 Expression Correlates with Breast Cancer Metastasis in MDA-MB-231 Cells In Vitro, In a Mouse Xenograft Model and in Human Breast Cancer Tissues. Cancers (Basel), 2019. **11**(4).
161. Phillips, S.L., et al., Connexin 43 in the development and progression of breast cancer: What's the connection? (Review). Int J Oncol, 2017. **51**(4): p. 1005-1013.
162. Qin, H., et al., Retroviral delivery of connexin genes to human breast tumor cells inhibits in vivo tumor growth by a mechanism that is independent of significant gap junctional intercellular communication. J Biol Chem, 2002. **277**(32): p. 29132-8.
163. Elzarrad, M.K., et al., Connexin-43 upregulation in micrometastases and tumor vasculature and its role in tumor cell attachment to pulmonary endothelium. BMC Med, 2008. **6**: p. 20.

164. <Connexin distribution in the rabbit and rat ciliary body. A case for heterotypic epithelial gap junctions..pdf>.
165. <Intravascular origin of metastasis from the.pdf>.
166. Keidar, Z., et al., 68Ga-PSMA PET/CT in prostate cancer patients - patterns of disease, benign findings and pitfalls. Cancer Imaging, 2018. **18**(1): p. 39.
167. Dbouk, H.A., et al., Connexins: a myriad of functions extending beyond assembly of gap junction channels. Cell Commun Signal, 2009. **7**: p. 4.